SSCL-655

SSCL-655
December 1993
Distribution Category: 414

D. J. Larson

A Study of the HEB Longitudinal Dynamics

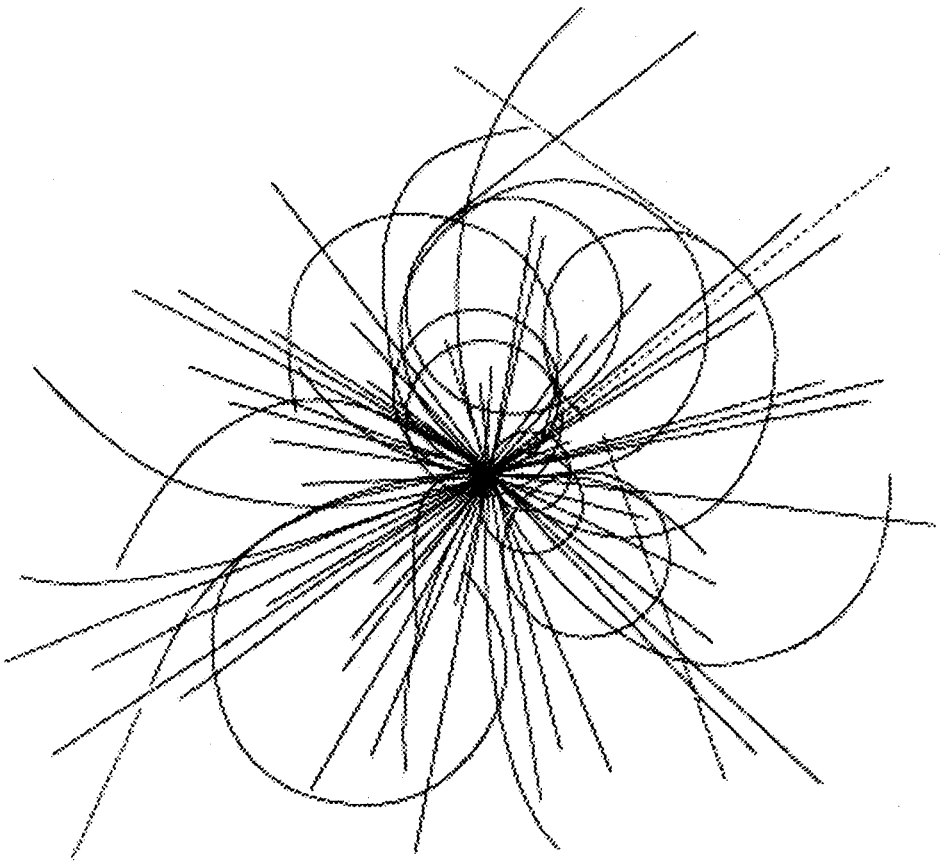

Superconducting Super Collider Laboratory

SSCL-655

A Study of the HEB Longitudinal Dynamics

D. J. Larson

Superconducting Super Collider Laboratory*
2550 Beckleymeade Ave.
Dallas, TX 75237

December 1993

*Operated by the Universities Research Association, Inc., for the U.S. Department of Energy under Contract No. DE-AC35-89ER40486.

A Study of the HEB Longitudinal Dynamics

D.J. Larson

Abstract

A study of the High Energy Booster (HEB) longitudinal dynamics is presented. Full derivations of ramp dependent longitudinal variables are given. The formulas assume that the input magnetic field and beam longitudinal emittance are known as a function of time, and that either the rf voltage or the rf bucket area are known as a function of time. Once these three inputs are specified, the formulas can be used to calculate values for all other longitudinal dynamics variables. The formulas have been incorporated into a single computer code named ELVIRA: Evaluation of Longitudinal Variables in Relativistic Accelerators. The ELVIRA code is documented here in detail. The ELVIRA code is used under two initial longitudinal emittance assumptions to plot ramp functions for the longitudinal dynamics design of the HEB as of May 5, 1992.

Key Words: Longitudinal Dynamics, ELVIRA, Ramp Dependent Variables: Magnetic Field; Rf Voltage; Longitudinal Emittance; Momentum; Energy; Rf Frequency; Rf Synchronous Phase; Synchrotron Frequency; Synchrotron Tune; Energy Spread; Momentum Spread; Bunch Length; Bucket Height; Bucket Width; Bucket Area; Moving Bucket Factor; Adiabaticity; Bunching Factor.

FOREWORD

PRESENT STATUS OF THE HEB DESIGN

This note gives the best estimate for the longitudinal dynamics of the HEB that is available at this time. The various longitudinal variable ramps presented in this work will soon be included as changes in the 3A and 3B specifications. Unfortunately, it is almost certain that some values for some of the various parameters will change before construction of the HEB, and when such changes occur a new version of this report will be prepared.

As discussed more fully below, the driving inputs for all of the work contained herein are 1) the magnet ramp; 2) the longitudinal bunch emittance; and 3) the desired bucket area to beam area ratio. Since these three inputs cause all changes in the longitudinal dynamical design, a brief description of present status and future outlook of each input will now be given.

- **Magnet Ramp**

The present magnet ramp has been the working design for quite some time, and it is unchanged from the original 3A specification.

Foreseen possible future changes in the ramp may include a faster ramp to allow a faster fill of the collider, changes in flat top and flat bottom duration, and changes in some of the times devoted to joining parabolas.

- **Longitudinal Bunch Emittance Cycle**

The present longitudinal bunch emittance cycle was arbitrarily chosen after a meeting which involved the MEB, HEB and Collider groups. The meeting was motivated by discussion with Jim Griffin, who suggested that earlier estimates of longitudinal emittance were probably too low to be realistic. Dr. Griffin has extensive experience with proton synchrotrons, and the design discussed herein uses numbers he suggests are in line with experience. These numbers are slightly larger than the ones that appear in the 3A spec. No future changes in the longitudinal emittance cycle are foreseen at this time.

- **The Bucket to Beam Area Ratio**

The present bucket to beam area ratio is chosen to be six, except for manipulation of the bucket required for bunch rotation. This ratio is close to the operating value of the Tevatron when the Tevatron operates in fixed target mode. It is felt that the Tevatron is a good experimental example for the HEB, since like the HEB it is a superconducting machine operating in the TeV energy range. The previous longitudinal dynamics design of the HEB did not use bucket to beam area as an input, rather the original 3A spec uses an arbitrary RF voltage cycle that led to a varying bucket to beam area ratio over the cycle, with the value ranging near 10. Thus, the ratio used here is somewhat less than that assumed in the original 3A spec. No future changes in the bucket to beam area ratio are foreseen at this time.

1.0 INTRODUCTION

This purposes of this note are to: 1) present graphical representations of the longitudinal phase space properties of the High Energy Booster (HEB) as a function of time; 2) present derivations of the formulas used to produce the graphs; and 3) document the computer code used to produce the graphs.

It would probably serve all three purposes better if a separate document were written for each of the above three tasks, and if time permits and demand warrants such an effort will be undertaken in the future.

The approach of this note is to discuss all issues in the order they appear in the computer code used to generate the graphical data. The computer code has been named ELVIRA, and the source code is located in the file elvira.f on the Euclid Sun workstation in the Superconducting Super Collider (SSC) computing complex. The input for the code is discussed in Section 2, and the output is discussed in Section 3. For every formula used to produce output a detailed derivation is given, followed by a description of where the coding can be found in the source code, which is in turn followed by a graphical representation of the specific longitudinal variable cycle within the present HEB design, and lastly a discussion of the longitudinal variable is given that lists specific numerical values for extreme points of the data.

ELVIRA uses formulas that are derived in MKSA units. However, some quantities are more readily (and traditionally) expressed in other units (such as nanoseconds or GeV). When other units are desired for the output, the formula derivation still uses the MKS units and conversion is done just prior to print out.

Occasionally approximations are made in the contained derivations, and there are a few rare places where a derivation is omitted entirely. Whenever an approximation or omission occurs, a line indicating

!APPROXIMATION!

or

!OMISSION!

makes note of such fact. These markings are to remind the reader of the approximate or omitted nature of the derivation. The approximations can be verified for accuracy, and the omissions filled in, with other computer codes. (ESME is one such code.)

2.0 INPUTS TO ELVIRA

This section of the note will discuss where the inputs to ELVIRA are entered (and hence where they can be changed for a new run). This section will also state the specific inputs relevant to the present HEB design. The output for the present HEB design is found in Section 3 of this document.

2.1 Machine and Physical Constants

The inputs to ELVIRA include physical constants, machine specific constants, arbitrary input cycles (such as the magnet ramp), calculational and plotting controls. In numeric expressions E is meant to be the usual FORTRAN meaning, 1E10 is equivalent to 1×10^{10}.

Physical constants used in ELVIRA are found on lines labeled 0001 to 0005 of the source code file, elvira.f:

1. The charge of the proton, denoted by:

$$Q = 1.60217733\text{E}{-19} \text{ Coulombs.} \tag{1}$$

2. The speed of light, denoted by:

$$C = 2.99792458E8 \text{ meters per second.} \tag{2}$$

3. The rest mass of the proton, denoted by:

$$MP = 1.6726231E{-}27 \text{ kg.} \tag{3}$$

4. The ratio of the circumference of a circle to its diameter, denoted by:

$$PI = 3.141592653589793238. \tag{4}$$

5. *PI* divided by 2 is coded into line 0005

$$PI02 = PI/2.$$

6. An often used conversion factor is the conversion between Joules and GeV, this is accomplished within the code by multiplying by a conversion factor located on the line labeled 0006:

$$CONV = 1./(Q*1.E9). \tag{5}$$

In addition to these physical constants written into the code itself, there are other constants that are entered through the file ELVIRA.IN. Some of the constants entered in ELVIRA.IN are machine specific constants that may change with design changes, or can be changed if the code is used for another machine, such as the Medium Energy Booster (MEB) or Collider.

Machine constants entered in the first line of the file ELVIRA.IN are:

1. The bending radius of the machine dipoles, denoted by:

$$RHO = 1001.32 \text{ meters.} \tag{6}$$

2. The energy at which the revolution frequency does not change with a small change in energy, known as the transition energy, denoted by:

$$GAMMAT = 34.47499. \tag{7}$$

3. The ratio of the rf frequency to the particle recirculation frequency, known as the harmonic number, denoted by:

$$H = 2160. \tag{8}$$

4. The circumference of the machine, denoted by:

$$CIRC = 10\,800 \text{ meters.} \tag{9}$$

2.2 Plotting and Calculational Controls

The plotting and calculational controls are input through the file ELVIRA.IN.

1. ELVIRA calculates the various parameters for specific times. $T = 0$ is defined as the point in the rf ramp where the flat injection ramp begins. ELVIRA then outputs data

every time an interval DT passes (output occurs at $T = 0$, $T = DT$, $T = 2DT$, $T = 3\,DT$, *etc.*) here:

$$DT = 0.1 \text{ seconds.} \tag{10}$$

2. ELVIRA is capable of specifying magnet ramps for either bipolar or monopolar machines. (A bipolar machine is one that has both a positive magnetic field ramp and a mirror image negative magnetic field ramp.) The switch is controlled by the variable *MODE*. *MODE* = 1 for monopolar and for the bipolar HEB:

$$MODE = 2. \tag{11}$$

3. ELVIRA is capable of using either the rf single pass effective peak voltage or the bucket area as an input. Which variable is treated as an input is controlled by the switch *VFLAG*. If the rf voltage is to be treated as an input, *VFLAG* = 1, but if bucket area is to be treated as an input, as it is in the HEB design,

$$VFLAG = -1. \tag{12}$$

2.3 What Ramp Functions are Controllable, *i.e.*, What Are the Other Inputs?

In dealing with the longitudinal variables, the quantities that are controllable are those of the rf system, namely the phase and amplitude of the rf, as well as the longitudinal emittance of the beam. Here the phase of the rf is defined to be $\phi = \arcsin(\Delta E/\mathrm{eV})$, where ΔE is the energy gained by the beam in a single pass, e is the charge on the particles, and V is the single pass effective peak voltage of the rf cavities. (It is assumed here that the longitudinal emittance of the beam can be increased during the ramp cycle. More on this in Section 2.5 below.) There are thus three independent variables that can serve as inputs for the remaining longitudinal variables.

It may seem natural to use the rf voltage and phase, and the longitudinal emittance as code inputs. The longitudinal emittance is indeed used as one such input. But for the other two independent variables it is more desirable to specify the magnetic field ramp and the bucket area, and use those inputs to derive the voltage and phase required of the rf system. (The bucket area is the area in phase space that is capable of stably containing particles.) The magnet ramp is usually determined by considerations other than the rf system, such as hysteresis losses, or power supply capabilities, and it is therefore a constraint on the system that the rf system must meet. The bucket area must be larger than the longitudinal emittance of the beam, or particles will be lost. If the bucket area is too large however, longitudinal emittance growth or instabilities may occur. Therefore it is desirable to control the bucket area, and thus it is best to use the bucket area as the final arbitrary input when defining system parameters.

While in hindsight it is clear that it is best to use the bucket area as an input, this was not done in the first derivation of the ramp functions for the SSC complex done by Miguel Furmann, nor is this done in the Fermilab control codes that calculate longitudinal variables of the ramp, nor was this done in the first version of ELVIRA. It was only after Jim Griffin made the above arguments that bucket area was incorporated as an input into ELVIRA. This has led to the present situation where either the voltage or the bucket area can be used as inputs to ELVIRA. In this way ELVIRA can be checked versus existing codes for accuracy by using a voltage input, or it can be used to derive longitudinal variables the better way by using a bucket area input.

The three independent inputs will now be discussed.

2.4 Defining the Magnetic Cycle

There are typically three regions of the magnetic ramp that contain beam: 1) A flat section of constant magnetic field exists for beam injection; 2) A linearly increasing field is used during particle acceleration;

and 3) A flat section of constant magnetic field exists for beam manipulations needed just prior to extraction. The second constant magnetic field region is called the "flat top".

In addition to the three regions of the magnetic ramp that contain beam, the magnetic ramp must be reset to its initial condition just prior to the next (half) cycle. And, since the HEB is a bipolar accelerator, there must be a symmetric ramp for the second half of the cycle. For the HEB, the magnetic field decreases linearly to zero after the flat top, pauses for a short time at zero, and finally decreases to the value required for injection into the next half of the cycle.

The constant (flat) regions of the field and the linear connections between the flat regions cannot be abruptly joined. An abrupt change in magnetic field would lead to an abrupt change in the required synchronous particle momentum, and this implies an abrupt change in the rf voltage and/or synchronous phase. Abrupt changes in rf voltage or synchronous phase can lead to unwanted longitudinal emittance increase, or, in the worst case, beam loss. For this reason, parabolas are specified to gradually join flat regions to linearly increasing regions. Parabolas are not required when there is no beam in the ring, but the code allows parabolic inputs at all joinings, and the ones that don't need parabolas can simply be set to zero.

In general then, there are many input parameters that need to be specified in order to fully specify the magnetic ramp. The values of the field at injection and at extraction are required. The value of the field at the pause (zero for the bipolar HEB) is also needed. The amount of time the field is to remain at the pause, injection and extraction levels is required. The amount of time desired for the up (accelerating) ramp, down ramp, and pre-injection ramp is also required as inputs. Lastly, the amount of time needed for the joining parabolas must be put into the program as an input. The second half of the bipolar cycle need not be specified, as symmetry is used to arrive at the specifications.

The inputs for the magnet ramp are found in the file ELVIRA.IN on lines 3, 4, and 5. The magnetic field at any given time is calculated by the code ELVIRA at regular intervals, with the coding located in the lines between the labels 100 and 250 in the source code elvira.f.

The time specified for the magnetic field to remain flat for injection, $TIN1$, the time specified for the parabolic joining of the injection flat and the up ramp, $P1$, and the value of the magnetic field at injection, $B1$, are the first three inputs on line 3 in ELVIRA.IN:

$$TIN1 = 20.\ \text{seconds},\ P1 = 1.5\ \text{seconds},\ B1 = 0.666251189\ \text{Tesla}. \tag{13}$$

The time specified for the up ramp, $TIN2$, and the time specified for the parabolic joining of the up ramp to the flat top, $P2$, are the last two inputs on line 3:

$$TIN2 = 100.\ \text{seconds},\ P2 = 1.5\ \text{seconds}. \tag{14}$$

The time specified for the magnetic field to remain flat for beam manipulation and ejection, $TIN3$, the time specified for the parabolic joining of the ejection flat and the down ramp, $P3$, and the value of the magnetic field at ejection, $B3$, are the first three inputs on line 4 in ELVIRA.IN:

$$TIN3 = 6.5\ \text{seconds},\ P3 = 1.5\ \text{seconds},\ B3 = 6.66251189\ \text{Tesla}. \tag{15}$$

The time specified for the down ramp, $TIN4$, and the time specified for the parabolic joining of the down ramp to the pause, $P4$, are the last two inputs on line 4:

$$TIN4 = 112.5\ \text{seconds},\ P4 = 0.0\ \text{seconds}. \tag{16}$$

The time specified for the magnetic field to remain flat at the pause, *TIN*5, the time specified for the parabolic joining of the pause flat and the pre-injection ramp, *P*5, and the value of the magnetic field at pause, *B*5, are the first three inputs on line 5 in ELVIRA.IN:

$$TIN5 = 2.5 \text{ seconds}, P5 = 0.0 \text{ seconds}, B5 = 0.0 \text{ Tesla}. \tag{17}$$

The time specified for the pre-injection ramp, *TIN*6, and the time specified for the parabolic joining of the pre-injection ramp to the injection flat, *P*6, are the last two inputs on line 5:

$$TIN6 = 10.5 \text{ seconds}, P6 = 1.5 \text{ seconds}. \tag{18}$$

In addition to calculating the magnetic field as a function of time, some quantities of interest also require knowledge of the derivative of the magnetic field as a function of time. For flat regions, this is obviously zero, linearly increasing regions have a constant dB/dt, and regions of parabolic change in B have a linear change in dB/dt. The coding for calculating dB/dt is found between the lines labeled 0120 and 0250 in the source code elvira.f.

2.5 Defining the Longitudinal Emittance Cycle

During the acceleration of the proton beam the relative energy spread $\Delta E/E$ of the beam will naturally shrink. If $\Delta E/E$ gets too small the beam will become unstable. In order to avoid beam instabilities the present SSC design calls for a planned increase in the longitudinal phase space area over time. How this increase is to be provided is not specified at the moment, but it may be done by rf noise, periodically and abruptly varying the rf voltage, shaking the phase during acceleration or storage, or the use of barrier buckets at injection or ejection. The longitudinal emittance is thus another parameter of the longitudinal dynamics that is an arbitrary input into ELVIRA.

The inputs for the longitudinal emittance cycle are found in the file ELVIRA.IN on line 9. The longitudinal emittance is calculated by ELVIRA at regular intervals, with the coding located in the lines between the labels 120 and 200 in the source code elvira.f. It is assumed that the emittance will remain flat during the injection flat, increase linearly during the acceleration ramp, and remain flat during the flat top until ejection.

The phase space area during injection, *EPL*1 and the phase space area during the flat top, *EPL*2 as found on line 9 in ELVIRA.IN are

$$EPL1 = 0.33 \text{ eV-seconds and } EPL2 = 0.66 \text{ eV-seconds}. \tag{19}$$

(Note that in Miguel Furmann's work he used *EPL*1 = 0.075 eV-seconds and *EPL*2 = 0.66 eV-seconds).

Note that *EPL*1 and *EPL*2 are entered in non-MKS units, eV-seconds, rather than the MKS units Joule-seconds, in order to conform to the usual notation (also, the values are closer to unity when expressed in this way). A conversion of units is done prior to using the input within the code, so the code can do all calculations in MKS units.

2.6 Defining the Rf Voltage Cycle or the Bucket Area

As discussed above in Section 2.3, either the rf voltage or the bucket area cycle can be used as an arbitrary input. Also discussed in Section 2.3 is the flag that tells the code which input to use. Section 2.6.1 will first discuss the possibility of using rf voltage as an input, as was done by Miguel Furmann. Section 2.6.2 will discuss the possibility of using bucket area as an input, as was proposed by Jim Griffin.

2.6.1 Using the Rf Voltage Cycle as the Arbitrary Input

If rf voltage is to be used as the last arbitrary input, the flag *VFLAG* should be set to 1 as discussed in Section 2.3. Miguel Furmann's design for the HEB rf system used voltage inputs that will be explained in this subsection.

The voltage related quantity of interest for the longitudinal particle dynamics is the amount of energy a particle will get during a single pass through the acceleration cavities. Therefore it is best to use a "single pass effective peak voltage" (SPEPV) that is related to, but not the same as, the actual peak voltage within an individual cavity. The SPEPV will be somewhat less than N times the peak voltage within an individual cavity due to transit time effects. (N is the number of cavities employed in the ring. As the particles traverse an individual cavity, the voltage will not remain fixed, and this alters the peak effective voltage.) Even though the SPEPV will not be exactly the same as the sum of the voltages of the cavities employed, it is usual to refer to the SPEPV as the "rf voltage," and this nomenclature will be adopted from this point forward.

For the ELVIRA computer code it is assumed that the rf voltage is constant during injection, increases linearly during the parabolic portion of the magnet ramp just prior to the linear momentum increase, and then remains constant at the new higher value until just before beam ejection.

The present design for the Collider calls for an rf system within the Collider that operates with parameters necessitating a shorter proton bunch than what can be achieved in the HEB with a constant rf voltage. The plan for shortening the bunch is to use a "bunch rotation" by slowly decreasing the rf voltage, which has the effect of slowly increasing the bunch length. The rf voltage is planned to remain at the low level for a short time while timing is set for the transfer. Then, when the timing is correct, the rf voltage is to be suddenly increased. A sudden increase has the effect of starting an oscillation in the bunch length. When the oscillation reaches the point of shortest bunch length, the kickers will be energized to transfer the bunch into the Collider.

Although the change in rf voltage from a constant to a linear ramp can not be done instantly in an actual physical device, it is assumed in ELVIRA that the change can be done over a time that is short with respect to the changing of the quantities of interest. (The time scale of interest for the longitudinal dynamics is the period of synchrotron oscillations. The synchrotron oscillations are discussed below in Section 3.9. The period of the synchrotron oscillations in the HEB is of the order of 100 milliseconds, and it should be possible to arrange a change in rf voltage orders of magnitude more quickly than this time scale.)

The inputs for the rf voltage cycle are found in the file ELVIRA.IN on lines 6 and 7. The rf voltage is calculated by ELVIRA at regular intervals, with the coding located in the lines between the labels 120 and 200 in the source code elvira.f.

The timing of the rf voltage changes is entered in line 6, while the values of the various voltages are entered in line 7. Line 6 contains: 1) the amount of time the rf voltage remains at the acceleration level during the flat top, *TVIN*1; 2) the time interval used in the slow voltage decrease, *TVIN*2; 3) the time the rf voltage remains at the lowest level for the setting of the timing, *TVIN*3; and 4) the time associated with the fast rise of the rf voltage, *TVIN*4. To compare with Miguel Furmann's work the necessary inputs are:

$$TVIN1 = 3.0 \text{ secs.}, \; TVIN2 = 1.0 \text{ secs.}, \; TVIN3 = 0.5 \text{ secs.}, \; TVIN4 = 0.1 \text{ secs.} \tag{20}$$

Line 7 contains the value of the rf voltage during injection, $V1$, the value of the rf voltage during the acceleration cycle and beginning of the flat top, $V2$, the value of the rf voltage at the end of the slow voltage decrease, $V3$, and the value of the rf voltage at ejection, $V4$. To compare with Miguel Furmann's work the necessary inputs are:

$$V1 = 400\,000 \text{ Volts (V)}, \; V2 = 1\,600\,000 \text{ V}, \; V3 = 80\,000 \text{ V}, \; V4 = 1\,500\,000 \text{ V}. \tag{21}$$

2.6.2 Using the Bucket Area Cycle as the Arbitrary Input

If bucket area is to be used as the last arbitrary input, the flag *VFLAG* should be set to –1 as discussed in Section 2.3. The present design for the HEB rf system (described here) uses the bucket area inputs that will be explained in this subsection.

The bucket area is calculated by ELVIRA at regular intervals, with the coding located in the lines between the labels 120 and 200 in the source code elvira.f. It is assumed that the bucket area will remain flat during the injection flat, change linearly during the acceleration ramp, and remain flat during the flat top until the bunch rotation is to take place. ELVIRA allows the capability to calculate the required rf voltage and resulting adiabaticity of a bunch rotation by entering four timing changes of the bucket area during the flat top.

The inputs for the bucket area cycle are found in the file ELVIRA.IN on lines 6 and 8. Line 6 enters the amount of times, *TVIN*1, *TVIN*2, *TVIN*3 and *TVIN*4 that are allotted for various bucket area manipulations at the flat top. *TVIN*1 is the time that the bucket area remains at *ABKT*2 during the flat top. The amount of time reserved to slowly decrease the bucket area to *ABKT*3 is entered as *TVIN*2. The time that the bucket area remains flat at *ABKT*3 is entered as *TVIN*3 and the time allotted for the increase of the bucket area to *ABKT*4 is entered as *TVIN*4. For the present design of the HEB used in this report:

$$TVIN1 = 3.0 \text{ secs.}, \; TVIN2 = 1.0 \text{ secs.}, \; TVIN3 = 0.5 \text{ secs.}, \; TVIN4 = 0.1 \text{ secs.} \tag{22}$$

Line 8 contains: 1) the value of the bucket area during injection, *ABKT*1; 2) the value of the bucket area when the magnet ramp first reaches the flat top, *ABKT*2; 3) the value of the bucket area just prior to the increase required for bunch rotation, *ABKT*3; and 4) the bucket area which is increased for bunch rotation, *ABKT*4. For the present design of the HEB used in this report:

$$ABKT1 = 2 \text{ eV-s}, \; ABKT2 = 4 \text{ eV-s}, \; ABKT3 = 3.5 \text{ eV-s}, \; ABKT4 = 16.5 \text{ eV-s}. \tag{23}$$

As with the case of the longitudinal emittance, the bucket area is entered in the non-MKS units eV-seconds. A conversion of the bucket area into the units of Joule-seconds is done prior to the calculational portion of the code, so that the code can do all calculations in MKS.

3.0 OUTPUTS OF THE CODE ELVIRA FOR THE PRESENT HEB DESIGN

This section will present graphs of the various quantities of interest for the longitudinal dynamics of the present HEB design. Each subsection will also contain a brief derivation of the formula used in ELVIRA for the particular quantity of interest, mention where in the source code the coding can be found, and end with a discussion of the plotted data. Approximations and omissions in the derivations are prominently labeled.

3.1 The Magnetic Field Cycle

Derivation of Formula

No derivation is required for the output value, as the magnetic field ramp is an arbitrary input into ELVIRA. See Section 2.4 for the input discussion.

Location of Coding in elvira.f

As discussed in Section 2.4, the magnetic field cycle is encoded between the lines labeled 0100 and 0250 in the source file elvira.f. Printing is coded into the line labeled 0240.

Graphical Representation

Figure 1 depicts the magnetic field cycle of the HEB.

Discussion

As seen in Figure 1, the magnetic field is constant, at 0.66625 Tesla for the first 20 seconds, has a parabolic match to the linear ramp for the next 1.5 seconds, linearly increases for the next 100 seconds, has a parabolic match to the flat top for the next 1.5 seconds, has a flat top magnetic field of 6.6625 Tesla for the next 6.5 seconds, has a parabolic match to the down ramp for the next 1.5 seconds, decreases linearly for the next 112.5 seconds, pauses at zero field for 2.5 seconds, has a linear ramp to the next injection flat of 10.5 seconds, and a parabolic match to the flat injection field over the next 1.5 seconds. The second (negative) half of the cycle is a symmetric reproduction of the first half of the cycle.

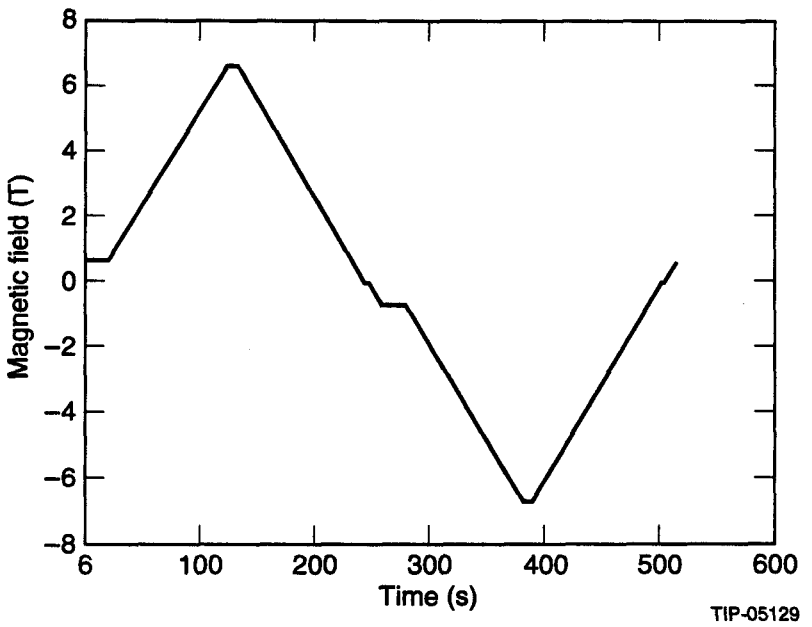

Figure 1. The HEB magnetic field cycle.

3.2 The Rf Voltage Cycle

Derivation of Formula

In the case where the voltage is an arbitrary input into ELVIRA no derivation is required for this output value. For this case, see Sections 2.3 and 2.6.1 for the input discussion.

In the case where the voltage is derived from the input bucket area, which is the case considered here, a derivation is needed, but the derivation is postponed until Section 3.22, which discusses the bucket area cycle for the HEB. For this case, see Sections 2.3 and 2.6.2 for the input discussion, and Section 3.22 for the formula derivation.

Location of Coding in elvira.f

If the rf voltage is entered as an input, the coding for the rf voltage cycle is found between the lines labeled 0120 and 0200 in the source file elvira.f. The rf voltage units are transformed from Volts to Megavolts in line 0310 for printing purposes, and printing is coded into line 0320.

If the bucket area is entered as input, the coding for the rf voltage is found between the lines labeled 0520 and 0710 in the source file elvira.f. The rf voltage units are transformed from Volts to Megavolts in line 0690 for printing purposes, and printing is coded into line 0700.

Graphical Representation

Figure 2 depicts the rf voltage cycle of the HEB.

Discussion

As seen in Figure 2, the rf voltage is constant at 123 300 Volts during the 20 second injection flat of the magnetic ramp, increases to 1.21 Megavolts during the first parabolic ramp, decreases to 1.02 Megavolts by the end of the acceleration ramp, decreases to 50 000 Volts during the second parabolic ramp, remains at 50 000 Volts until the beam is ready for bunch rotation, slowly decreases to 38 700 Volts during the adiabatic decrease in bucket area, and finally increases to 861 500 Volts to accomplish the bunch rotation. The rf voltage then stays at 861 500 Volts until ejection.

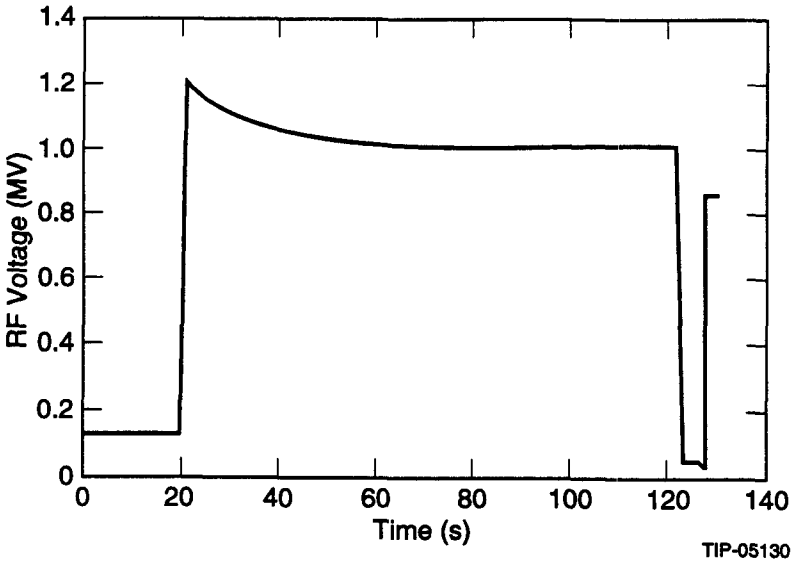

Figure 2. The HEB rf voltage cycle.

3.3 Longitudinal 95% Phase Space Area Evolution in the HEB

Derivation of Formula

No derivation is required for this output value, as the longitudinal 95% phase space area evolution is an arbitrary input into ELVIRA. See Section 2.5 for the input discussion.

Location of Coding in elvira.f

As discussed in Section 2.5, the coding for the longitudinal phase space cycle is found between the lines labeled 0120 and 0200 in the source file elvira.f. Printing is coded in line 0340. As discussed in Section 2.5, a conversion to MKS is done on line 0345.

Graphical Representation

Figure 3 depicts the longitudinal 95% phase space area evolution in the HEB.

Discussion

As seen in Figure 3, the longitudinal emittance is constant at 0.33 eV-seconds for the first 21.5 seconds, linearly increases during the 100 second acceleration ramp to 0.66 eV-seconds, and then remains constant at 0.66 eV seconds until ejection.

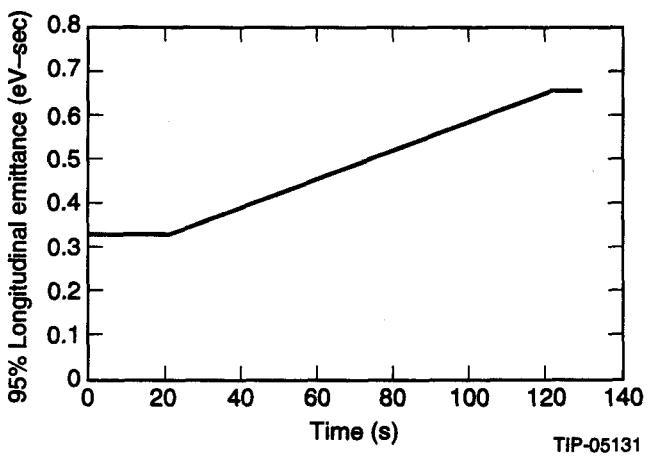

Figure 3. The HEB 95% longitudinal emittance cycle.

3.4 The Momentum Cycle

Derivation of Formula

It is an empirical observation that $F = \gamma ma$ for perpendicularly applied forces, where F is the force, m the (rest) mass of the particles, a the acceleration of the particles and γ the Larmor-Lorentz factor, $\gamma = (1 - \beta^2)^{-1/2}$, $\beta = v/c$ where c is the velocity of light and v is the velocity of the particles. Another empirical observation is that $F = QvB$ for magnetic fields of strength B imposed upon particles containing a charge Q, if those particles move with a velocity v in the frame where B is measured, and if the direction of v is perpendicular to the direction of B, as is the case here. The acceleration of a particle moving in a circular path is readily derived to be $a = v^2/r$, where r is the bend radius. Thus, $\gamma mv^2/r = QvB$, or $\beta\gamma mc = p = QBr$. The momentum is thus a simple constant times the magnetic field, when the bending radius is assumed constant. (It is assumed the particles will lie in the center of the dipole chambers for acceleration. This will be experimentally arranged by using beam position monitors in a dispersive section along with feedback to keep the beam in the center of the pipes.) Thus, the code uses:

$$p = QBr \tag{24}$$

where Q is a physical constant, r is a machine specific constant, and B is an arbitrary input discussed in Section 2.4.

Location of Coding in elvira.f

The coding for the momentum cycle is found on the line labeled 0350 in the source file elvira.f, a conversion of units is done on the line labeled 0360 so as to print out the momentum in units of GeV/c, and printing is coded into the line 0370.

Graphical Representation

Figure 4 depicts the HEB momentum cycle.

Discussion

As seen in Figure 4, the momentum cycle in the HEB is flat for the first 20 seconds at the injection level of 200 GeV/c, joins to the ramp with a 1.5 second parabola, linearly increases over the next 100 seconds, joins to the flat top with a 1.5 second parabola, and remains at the flat top level of 2000 GeV/c until ejection.

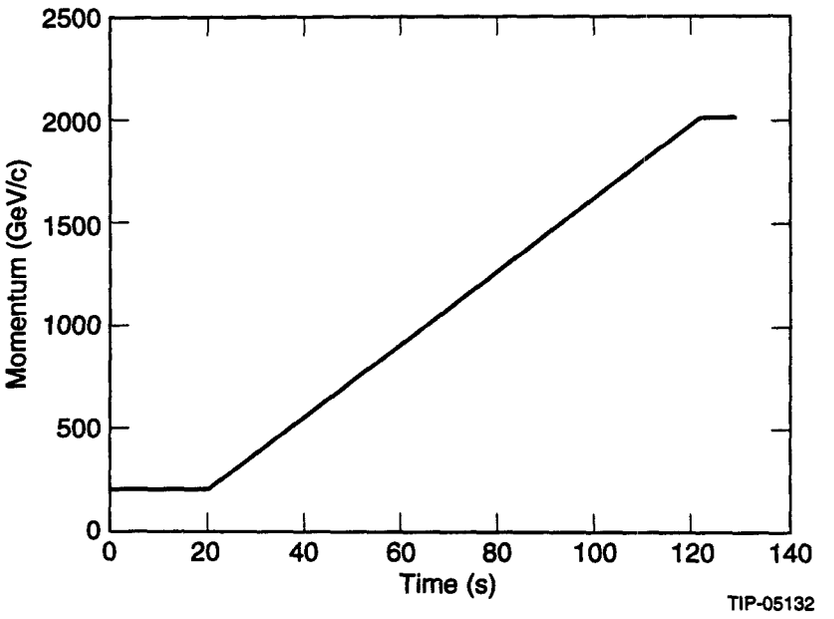

Figure 4. The HEB momentum cycle.

3.5 The Energy Cycle

Derivation of Formula

It is an empirical observation that $E = (p^2c^2 + m^2c^4)^{1/2}$, where E is the particle energy, p the particle momentum, m the (rest) mass of the particle and c the velocity of light. Thus, the code uses

$$E = (p^2c^2 + m^2c^4)^{1/2} \tag{25}$$

where m and c are physical constants, and p is derived in Section 3.4.

Location of Coding in elvira.f

The coding for the energy cycle is found on the line labeled 0380 in the source file elvira.f, a conversion of units is done on the line labeled 0390 so as to print out the energy in units of GeV, and printing is coded into the line 0400.

Graphical Representation

Figure 5 depicts the HEB synchronous energy cycle.

Discussion

As seen in Figure 5, the energy cycle in the HEB is flat for the first 20 seconds at the injection level of 200 GeV, joins to the ramp with a 1.5 second parabola, linearly increases over the next 100 seconds, joins to the flat top with a 1.5 second parabola, and remains at the flat top level of 2000 GeV until ejection.

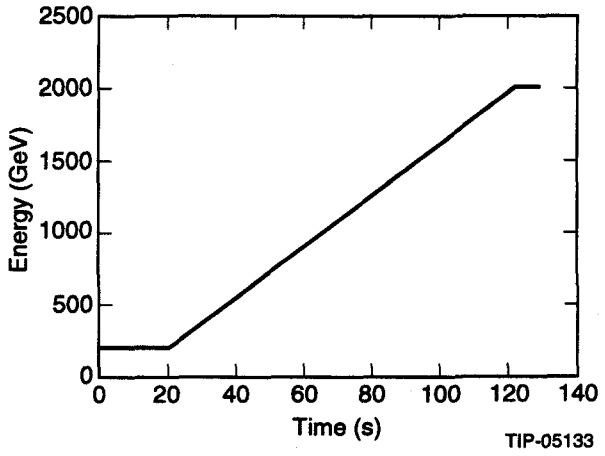

Figure 5. The HEB energy cycle.

3.6 The Rf Frequency Cycle

Derivation of Formula

The frequency of revolution for particles stored in the HEB will be the speed of the particles divided by the circumference of the particle trajectory, $f_0 = v/C$, where f_0 is the revolution frequency, C is the circumference of the particle trajectory and v is the particle speed. The particle speed is determined by the energy through the relation $v/c = \beta = (1 - 1/\gamma^2)^{1/2}$, where γ is the ratio of the total particle energy to the rest energy of the particle, $\gamma = E/mc^2$, where E is the particle energy, m the (rest) mass of the particle, and c the speed of light.

The rf frequency is an integer, called the machine harmonic number, multiplied by the revolution frequency, $f_{RF} = hf_0$, where f_{RF} is the rf frequency and h is the harmonic number. Thus, the code uses

$$f_{RF} = \frac{h \times v}{C} \text{ where } v = c \times \left(1 - \frac{m^2c^4}{E^2}\right)^{\frac{1}{2}} \text{ (Note that } \beta = v/c.) \tag{26}$$

where C and h are machine specific inputs, c and m are physical constants and E is derived in Section 3.5.

Location of Coding in elvira.f

The coding for the rf frequency cycle in the HEB is found on the lines labeled 0410 through 0470 in the source file elvira.f. Line 0410 codes for γ, Line 0420 codes for β, line 0440 codes for f_0, and line 0450 codes for f_{RF}. Since the rf frequency varies only slightly during the HEB cycle, the relevant quantity of interest is the deviation of the rf frequency from 59.957 MHz during the cycle, and it is desired that the units of this difference be kHz for the printout. The line labeled 0460 prepares the data in such a form for printing, and the line labeled 0470 codes for the printing.

Graphical Representation

Figure 6 depicts the HEB rf frequency cycle.

Discussion

As seen in Figure 6, the rf frequency cycle in the HEB is flat for the first 20 seconds at 831.8 Hz greater than 59.957 MHz, and then rises during the acceleration cycle to a level of 1485 Hz greater than 59.957 MHz at the flat top.

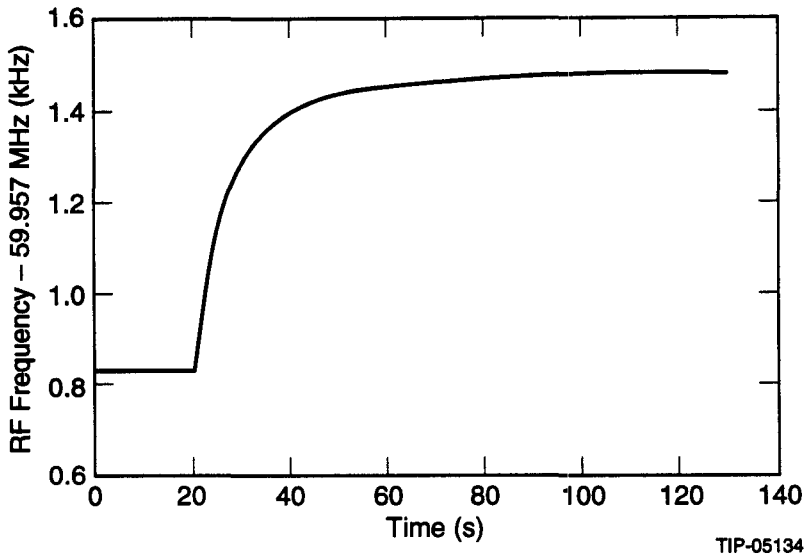

Figure 6. The HEB rf frequency cycle.

3.7 The $V\sin\phi_s$ Cycle

Derivation of Formula

A definition of the voltage between two points is $V = \Delta E/Q$, where ΔE is the energy gained by a particle of charge Q during its passage between the two points. The rf voltage is either an arbitrary input into the code ELVIRA, as is described in Section 2.6.1 above, or it is derived from an input bucket area, as is discussed in Section 3.22 below. Since the voltage within the cavities oscillates in time, the energy change experienced by a particle during a single pass will depend on the phase of the rf voltage during the transit. $V\sin\phi_s$ is defined here to be the energy increment given to the particles in a single pass through the rf cavities divided by the charge on the particles.

The energy increment required on any given pass through the rf cavities is determined by the energy cycle. As discussed in Section 3.5, the energy, E, is related to the momentum, p, by

$$E = (p^2c^2 + m^2c^4)^{1/2} . \tag{27}$$

Here m is the (rest) mass of the particle and c is the speed of light. Both the energy and the momentum are functions of time. Differentiating with respect to time leaves

$$dE/dt = (pc^2/E)(dp/dt). \tag{28}$$

Noting that the energy is defined as $E = \gamma mc^2$ and that the momentum is defined as $p = \beta\gamma mc$, where $\beta = v/c$, v is the velocity of the particles and $\gamma = (1 - \beta^2)^{-1/2}$, leaves

$$dE/dt = (\beta c)(dp/dt). \tag{29}$$

It is derived above in Section 3.4 that $p = QBr$, or $dp/dt = (Qr)(dB/dt)$, so

$$dE/dt = (\beta cQr)(dB/dt). \tag{30}$$

Now $V\sin\phi_s$ is defined through $\Delta E = QV\sin\phi_s$, where ΔE is the energy increment in one pass through the rf cavities and Q is the charge of the particles. The time required for the beam particles to make one revolution is the inverse of the frequency of particle revolution, $\Delta t = 1/f_0$, where f_0 is derived above in Section 3.6. Therefore $\Delta E/\Delta t = f_0QV\sin\phi_s$, and by setting $\Delta E/\Delta t = dE/dt$, and rearranging

$$V\sin\phi_s = (dE/dt)/(Qf_0) \text{ , where } dE/dt = (\beta cQr)(dB/dt), \tag{31}$$

where Q and c are physical constants, r is a machine specific constant, β and f_0 are calculated in the program as discussed in Section 3.6, and dB/dt is calculated in the program during the input of the magnetic field data, as discussed in Section 2.4.

Location of Coding in elvira.f

The coding for calculating dE/dt is found on the line labeled 0430 in the source code elvira.f, while the coding for $V\sin\phi_s$ is found on line 0480, the output is converted from V to MV on line 0490, and the printing is coded into line 0500.

Graphical Representation

Figure 7 depicts the HEB $V\sin\phi_s$ cycle.

Discussion

As seen in Figure 7, $V\sin\phi_s$ is zero during injection (as the beam must remain at the constant injection energy) increases during the parabolic ramp of the magnets to 638 900 Volts, remains flat at a level of 638 900 Volts during the acceleration cycle, and then returns to zero during the parabolic magnetic ramp just prior to flat top. $V\sin\phi_s$ remains at zero during the flat top except for any acceleration required by cogging. (The cogging acceleration can not be determined in advance.)

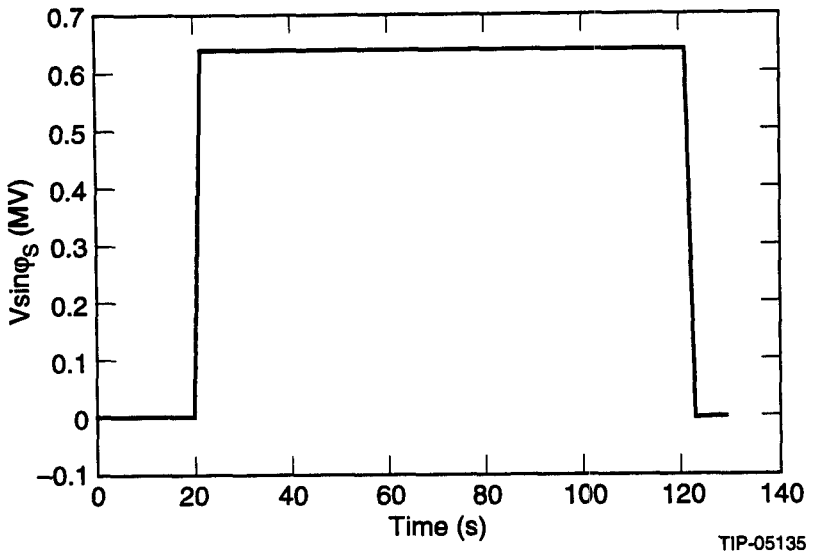

Figure 7. The HEB $V\sin\varphi_s$ cycle.

3.8 The ϕ_s Cycle

Derivation of Formula

Once $V\sin\phi_s$ is determined. as discussed in Section 3.7, with the input of V, as discussed in Section 2.6.1, or the derivation of V, as discussed in Section 3.22, ϕ_s is determined simply as the arcsine of $V\sin\phi_s/V$:

$$\phi_s = \text{arcsine}(V\sin\phi_s / V) \quad \text{(for machines below transition)} \tag{32}$$

where $V\sin\phi_s$ is computed in the program as derived in Section 3.7, and V is either an arbitrary input into the program as discussed in Section 2.6.1, or V is derived from an input bucket area as discussed in Section 3.22. However, the arcsine has two roots, and the correct root must be specified. If the machine is below transition, the above formula is appropriate, for machines above transition the relation is:

$$\phi_s = \pi - \text{arcsine}(V\sin\phi_s / V) \quad \text{(for machines above transition).} \tag{33}$$

Location of Coding in elvira.f

ELVIRA uses the variable $g = \sin\phi_s$. The coding for $\sin\phi_s$ is found on the lines labeled 0530 through 0640 in the source file elvira.f for the case where the voltage is determined from an input bucket area (see Section 3.22 for a detailed discussion of this portion of the code). The coding for $\sin\phi_s$ is found on line 0720 for the case where the rf voltage is treated as an arbitrary input. The coding for the ϕ_s cycle is found on the lines labeled 0820–0860 in the source file elvira.f, a conversion to degrees is done on the line labeled 0870, printing is coded into the line 0880.

Graphical Representation

Figure 8 depicts the HEB ϕ_s cycle.

Discussion

As seen in Figure 8, ϕ_s is 180 degrees during injection (as the beam must remain at the constant injection energy) decreases during the parabolic ramp of the magnets, ranges between 148.1 and 140.9 degrees during the acceleration cycle, and then returns to 180 degrees during the parabolic magnetic ramp just prior to flat top. ϕ_s remains at 180 degrees during the flat top except for any acceleration required by cogging. (The cogging acceleration can not be determined in advance.)

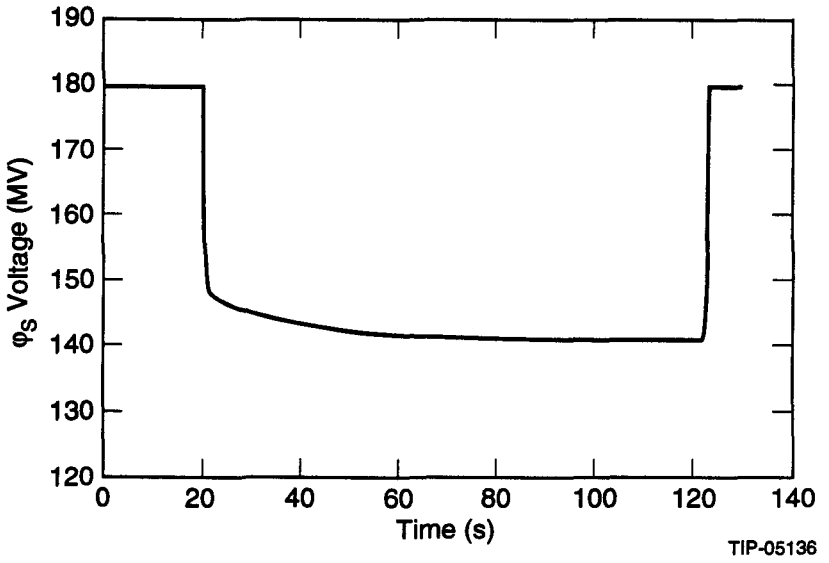

Figure 8. The HEB φ_s cycle.

3.9 The f_s Cycle

Derivation of Formula

Up to this point the discussion has proceeded as if all particles in the beam will have the same energy upon entry into the rf cavity, and that the phase of the rf upon entry will be the same for all particles in the beam. The presentation has been concerned with what is known as the synchronous energy and phase. In actuality the beam particles will have a spread of energies, and they will enter the rf cavity over a range of times corresponding to a spread in phase. In order to assure that the entire bunch of particles is accelerated and remains in the ring, it is necessary that small deviations from the central energy and phase exhibit stable oscillations about the central (synchronous) energy and phase. This section is concerned with a calculation of the frequency of those oscillations, called synchrotron oscillations.

Due to the discontinuous nature of the rf acceleration, the literature usually calculates the frequency of synchrotron oscillations with respect to the number of such oscillations per turn, and then it is usual to convert to the number of oscillations per second. Here, the derivation will find the number of oscillations per second directly. But the discontinuous nature of rf acceleration in a synchrotron must come into the derivations. Here, the derivation will proceed by investigating the energy change per single orbit period, $\Delta E/\Delta t_s$ and the phase change per single orbit period, $\Delta\phi/\Delta t_s$. The discontinuous change in energy will then be equated to a continuous energy change for the analysis.

As discussed above in Section 3.7, the energy gained by a particle on the synchronous orbit is determined by $\Delta E_s/\Delta t_s = f_0 Q V \sin\phi_s$, where ΔE_s is the synchronous energy gain in a single pass, $\Delta t_s = 1/f_0$ is the time required for the synchronous particle to make one orbit, f_0 is the synchronous revolution frequency, Q is the charge on the particle, V is the rf voltage and ϕ_s is the synchronous phase derived in Section 3.8. The derivation used in Section 3.7 can be generalized for non-synchronous particles to yield

$$\Delta E/\Delta t_s = f_0 Q V \sin\phi, \tag{34}$$

where ΔE is the single pass energy change for an arbitrary particle and ϕ is the phase of the rf when the arbitrary particle passes. Subtracting the equation for the synchronous orbit from the equation for the arbitrary particle leaves

$$(\Delta E - \Delta E_s)/\Delta t_s = f_0 Q V(\sin\phi - \sin\phi_s). \tag{35}$$

The difference between the arbitrary particle's energy change and the synchronous energy change is equal to the change in the difference between the arbitrary particle's energy and the synchronous energy, $(\Delta E - \Delta E_s) = (E_{n+1} - E_n) - (E_{sn+1} - E_{sn}) = (E_{n+1} - E_{sn+1}) - (E_n - E_{sn}) = \Delta(E - E_s)$. Defining the difference between the arbitrary particle's energy and the synchronous energy to be $\delta E = E - E_s$, and approximating the finite discontinuous energy change to a continuous energy change leaves

!APPROXIMATION!

$$d(\delta E)/dt = f_0 Q V(\sin\phi - \sin\phi_s). \tag{36}$$

The phase is determined by the time the particle enters the rf cavity. The voltage in the rf cavity has the form

$$V(t) = V\sin(2\pi f_{RF} t) = V\sin(2\pi t/\Delta t_{RF}) = V\sin\xi, \tag{37}$$

so a phase, ξ, has been defined,

$$\xi = 2\pi t/\Delta t_{RF}. \tag{38}$$

Equations (37) and (38) define $t = 0$ as one moment when $V(t) = 0$, and $dV(t)/dt > 0$. f_{RF} is the frequency of the rf, and Δt_{RF} is the period of the rf, $\Delta t_{RF} = 1/f_{RF}$.

With the phase as defined here, $\xi = 2\pi t/\Delta t_{RF}$, the phase will increase linearly with time. Yet the physics only depends on that part of the phase that is different from $2n\pi$, since the energy kick depends only on $V\sin\xi$, and $V\sin\xi = V\sin(\xi + 2n\pi)$, and it is therefore possible to discard $2n\pi$ from the phase with no change in the physics. It is the discarding of the $2n\pi$ that allows a definition of a fixed, synchronous phase. The synchronous phase is defined as that phase which causes the synchronous particle to always return to the rf cavity at the same, synchronous phase. This clearly can not be the case if the phase monotonically increases as defined in Equation (38). However, if a new phase, ϕ, is introduced such that the phase increase in one turn, $\Delta\phi$, is defined as

$$\Delta\phi = \Delta\xi - 2\pi\Delta t_s/\Delta t_{RF} = 2\pi(\Delta t - \Delta t_s)/\Delta t_{RF}, \tag{39}$$

where Δt_s is the orbit time for the synchronous particle, then, for the synchronous particle, $\Delta\phi = 0$, since for the synchronous particle $\Delta t = \Delta t_s$. The subtraction of $2\pi\Delta t_s/\Delta t_{RF}$ from $\Delta\xi$ is the same as a subtraction of $2\pi n$, only

if the ratio $\Delta t_s/\Delta t_{RF} = h$ is an integer. (This is the requirement for a synchronous phase, since when $\Delta t_s/\Delta t_{RF} = h$ is an integer, $\Delta\xi = 2\pi\Delta t_s/\Delta t_{RF} = 2\pi h$, and thus $V\sin\xi$ remains the same on each successive turn only if $\Delta t_s/\Delta t_{RF} = h$ is an integer.) The requirement $\Delta t_s/\Delta t_{RF} = h$ is built into the design of the accelerator or storage ring, and h is known as the harmonic number of the device.

Equation (39) states that the change in phase occurring in one turn is a function of the particle orbit time. The time required for a particle of arbitrary energy to make one orbit is $\Delta t = C/v$, where C is the circumference of the particle trajectory and v is the velocity of the particle. The time for the synchronous particle to make one orbit is $\Delta t_s = C_s/v_s$, where the s subscripts denote quantities related to the synchronous particle. The difference in orbit time between a particle of arbitrary energy and that of a particle with synchronous energy is

$$\Delta t - \Delta t_s = C/v - C_s/v_s. \tag{40}$$

Substituting Eq. (40) into (39) leaves an expression for the single turn phase change for a particle of arbitrary energy,

$$\Delta\phi = 2\pi(\Delta t - \Delta t_s)/\Delta t_{RF} = 2\pi h(\Delta t - \Delta t_s)/\Delta t_s = [2\pi h(C/v - C_s/v_s)]/[C_s/v_s]. \tag{41}$$

C and v can be rewritten as $C = C_s + \delta C$, $v = v_s + \delta v$. Thus,

$$\Delta\phi = 2\pi h([C_s + \delta C]/[v_s + \delta v] - C_s/v_s)/(C_s/v_s) = 2\pi h(v_s[C_s + \delta C] - [v_s + \delta v]C_s)/([v_s + \delta v]C_s)$$

$$= 2\pi h(v_s[\delta C] - [\delta v]C_s)/([v_s + \delta v]C_s) = 2\pi h\{[v_s/(v_s + \delta v)][\delta C/C_s] - [\delta v/(v_s + \delta v)]\} \tag{42}$$

which, to first order in the quantities $\delta C/C_s$ and $\delta v/v_s$ is

!APPROXIMATION!

$$\Delta\phi = 2\pi h(\delta C/C_s - \delta v/v_s). \tag{43}$$

The transition energy divided by the (rest) mass of the particles, γ_t, is defined through the relations

$$\delta C/C_s = \gamma_t^{-2}\delta p/p_s = \beta^{-2}\gamma_t^{-2}\delta E/E_s, \tag{44}$$

where δE is the energy difference between the synchronous energy and the particle with orbit circumference $C + \delta C$. The transition energy is largely determined by the transverse focusing properties of a machine, and it is left as an input into the code ELVIRA, so no further derivation of it will be given here.

Turning to the remaining term in (43), $\delta v/v_s$, note that differentiating the experimentally determined relation between energy and velocity, $E = (1 - v^2/c^2)^{-1/2}mc^2$, where m is the particle rest mass and c is the speed of light, leads to $\delta E = \delta v(v/c^2)(1 - v^2/c^2)^{-3/2}mc^2 = \delta v(\beta/c)\gamma^3 mc^2$, where $\beta = v/c$ and $\gamma = (1 - v^2/c^2)^{-1/2}$. Thus, $\delta E/E = \beta^2\gamma^2\delta v/v$, or

$$\delta v/v = \beta^{-2}\gamma^{-2}\delta E/E, \tag{45}$$

to first order in the small quantities $\delta v/v$ and $\delta E/E$.

!APPROXIMATION!

Substituting in the relation (45) for $\delta v/v_s$ and (44) for $\delta C/C_s$ leaves (43) as

$$\Delta\phi = 2\pi h(\delta C/C_s - \delta v/v_s) = 2\pi h(\beta^{-2}\gamma_t^{-2} - \beta^{-2}\gamma^{-2})\delta E/E_s = 2\pi h\eta\beta^{-2}\delta E/E_s\,, \tag{46}$$

where

$$\eta = (\gamma_t^{-2} - \gamma^{-2})\,, \tag{47}$$

and, by approximating that there is no change in the synchronous phase during the orbit, $\Delta\phi_s = 0$,

!APPROXIMATION!

$$\Delta(\delta\phi) = \Delta(\phi - \phi_s) = \Delta\phi - \Delta\phi_s = 2\pi h\eta\beta^{-2}\delta E/E_s\,. \tag{48}$$

Equation (48) makes use of the definition $\delta\phi = \phi - \phi_s$, as well as $(\Delta\phi - \Delta\phi_s) = (\phi_{n+1} - \phi_n) - (\phi_{sn+1} - \phi_{sn}) = (\phi_{n+1} - \phi_{sn+1}) - (\phi_n - \phi_{sn}) = \Delta(\phi - \phi_s)$. Equation (48) is an expression for the change in the phase difference between an arbitrary particle and the synchronous phase over one orbit. Thus, the time rate of change of $\delta\phi$ is

$$d(\delta\phi)/dt = \Delta(\delta\phi)/\Delta t_s = 2\pi h\eta\beta^{-2}\delta E/(E_s\Delta t_s) = 2\pi h\eta\beta^{-2}f_0\delta E/E_s\,. \tag{49}$$

(Note that a non-obvious approximation goes into Eq. (49). In the derivation of (48) the evaluation of the phase advance of an arbitrary particle is calculated for one turn of the arbitrary particle; while the phase advance of the synchronous particle is calculated for one turn of the synchronous particle. Thus, to state that the change in phase difference, $\Delta(\delta\phi)$, occurs over the time Δt_s is not exactly correct. The correct time rate of change for ϕ is determined by dividing the expression for $\Delta\phi$ given in Eq. (39) by Δt

$$d\phi/dt = \Delta\phi/\Delta t = 2\pi(\Delta t - \Delta t_s)/\Delta t\Delta t_{RF}\,, \tag{50}$$

By now defining $\Delta t = \Delta t_s + \delta\Delta t$, (50) can be re-expressed as

$$d\phi/dt = \Delta\phi/\Delta t = 2\pi\delta\Delta t/(\Delta t_s + \delta\Delta t)\Delta t_{RF}\,. \tag{51}$$

Expression (51) is the same as $d\phi/dt = \Delta\phi/\Delta t = 2\pi\delta\Delta t/\Delta t_s\Delta t_{RF}$ to first order in the small quantity $\delta\Delta t/\Delta t_s$. This first order expression is used to arrive at Eq. (49).)

!APPROXIMATION!

At this point there are now two coupled first order differential equations, (36) and (49).

$$d(\delta E)/dt = f_0QV(\sin\phi - \sin\phi_s). \tag{52}$$

$$d(\delta\phi)/dt = 2\pi h\eta\beta^{-2}f_0(\delta E)/E_s\,. \tag{53}$$

Differentiating the expression for $d(\delta\phi)/dt$ with respect to time leaves

$$d^2(\delta\phi)/dt^2 = (\delta E)(d[2\pi h\eta f_0/E_s\beta^2]/dt) + (2\pi h\eta f_0/E_s\beta^2)[d(\delta E)/dt]. \tag{54}$$

It is assumed that the first term is negligible (and this should be checked by a longitudinal particle tracking code). Substituting Eq. (36) into (54) leaves

$$d^2(\delta\phi)/dt^2 = (2\pi h\eta f_0^2 QV/E_s\beta^2)(\sin\phi - \sin\phi_s). \tag{55}$$

!APPROXIMATION!

$\sin\phi$ can be re-expressed as,

$$\sin\phi = \sin(\phi_s + \delta\phi) = \sin(\phi_s)\cos(\delta\phi) + \cos(\phi_s)\sin(\delta\phi) = \sin(\phi_s) + \cos(\phi_s)(\delta\phi). \tag{56}$$

The last step in Eq. (56) uses the approximations $\cos(\delta\phi) = 1$ and $\sin(\delta\phi) = (\delta\phi)$ for small values of $(\delta\phi)$.

!APPROXIMATION!

Substituting Eq. (56) into (55) results in a linear second order differential equation for $(\delta\phi)$:

$$d^2(\delta\phi)/dt^2 = (2\pi h\eta f_0^2 QV\cos\phi_s/E_s\beta^2)(\delta\phi). \tag{57}$$

Thus, provided all the approximations used in the derivation are sound, the time evolution second order differential equation for $\delta\phi$ is that of a simple harmonic oscillator. The solution is well known, and can be verified by substituting the solution back into the differential equation. The solution is:

$$\delta\phi = A\sin(\omega_s t + \psi)\ ,\ \text{with}\ \omega_s = (f_0/\beta)(-2\pi h\eta QV\cos\phi_s/E_s)^{1/2}. \tag{58}$$

A and ψ are constants determined by the initial phase and energy of the individual particle. (Note that a minus sign appears within the square root. For bounded motion it is thus required that $\eta\cos\phi_s$ be less than zero. This is the well known condition that requires $\cos\phi_s$ to be less than zero above transition, where $\gamma > \gamma_t$ and $\eta > 0$, and $\cos\phi_s$ to be greater than zero below transition, where $\gamma < \gamma_t$ and $\eta < 0$.) Thus, the equation used to calculate f_s is

$$f_s = \omega_s/2\pi = (f_0/\beta)(-h\eta QV\cos\phi_s/2\pi E_s)^{1/2}\ ,\ \text{with}\ \eta = \gamma_t^{-2} - \gamma^{-2}. \tag{59}$$

Q and π are physical constants, h and γ_t are machine specific constants, f_0, β and γ are derived in Section 3.6, E_s is derived in Section 3.5, V is either an input discussed in Section 2.6.1 or else V is derived from an input bucket area as discussed in Section 3.22, and ϕ_s is derived in Section 3.8.

Location of Coding in elvira.f

The coding η for is found on the line labeled 0510 in the source code elvira.f, the coding for the f_s cycle is found on line 0890 and printing is coded into line 0900.

Graphical Representation

Figure 9 depicts the HEB f_s cycle.

Discussion

As can be seen from Figure 9, the synchrotron frequency is flat during injection at 11.6 Hz, rises sharply during the first parabolic ramp of the magnetic field to 32.4 Hz, then decreases to 9.42 Hz during the acceleration ramp, decreases during the second parabolic ramp of the magnetic field to 2.38 Hz, pauses at 2.38 Hz to set the timing for transfer, decreases to 2.08 Hz during the adiabatic decrease of the bucket area, and suddenly increases to 9.80 Hz to accomplish the bunch rotation.

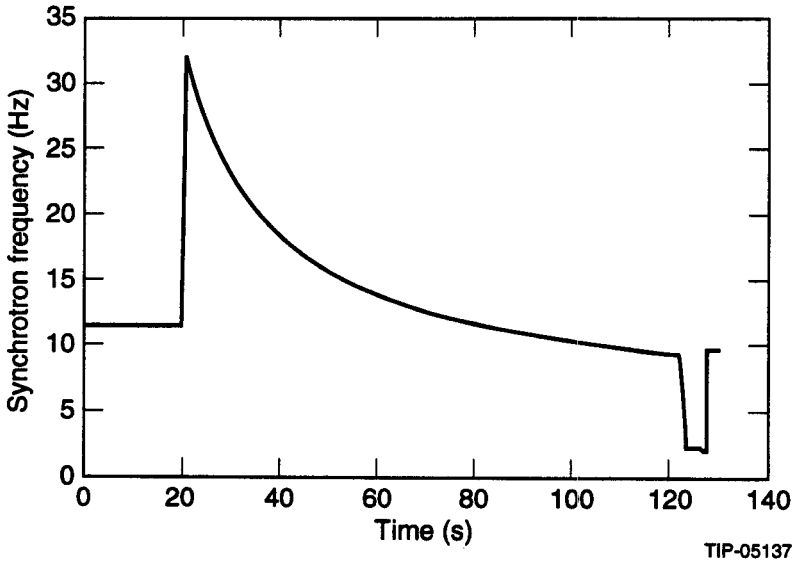

Figure 9. The HEB synchrotron frequency cycle.

3.10 The ν_s Cycle

Derivation of Formula

In addition to knowing the number of synchrotron oscillations per unit time, it is often desirable to know the number of synchrotron oscillations per orbit. This is simply determined by dividing the synchrotron frequency by the revolution frequency,

$$\nu_s = f_s/f_0 . \tag{60}$$

f_0 is derived in Section 3.6 and f_s is derived in Section 3.9.

Location of Coding in elvira.f

The coding for the ν_s cycle is found on the line labeled 0910 in the source file elvira.f, line 0915 multiplies ν_s by 1000 for clarity in plotting and printing is coded into the line 0920.

Graphical Representation

Figure 10 depicts the HEB synchrotron tune cycle.

Discussion

As can be seen from Figure 10, the synchrotron tune is flat during injection at 4.17×10^{-4}, rises sharply during the first parabolic ramp of the magnetic field to 1.17×10^{-3}, then decreases to 3.39×10^{-4} during the acceleration ramp, decreases during the second parabolic ramp of the magnetic field to 8.56×10^{-5}, pauses at 8.56×10^{-5} to set the timing for transfer, decreases to 7.49×10^{-5} during the adiabatic decrease in the bucket area, and suddenly increases to 3.53×10^{-4} to accomplish the bunch rotation.

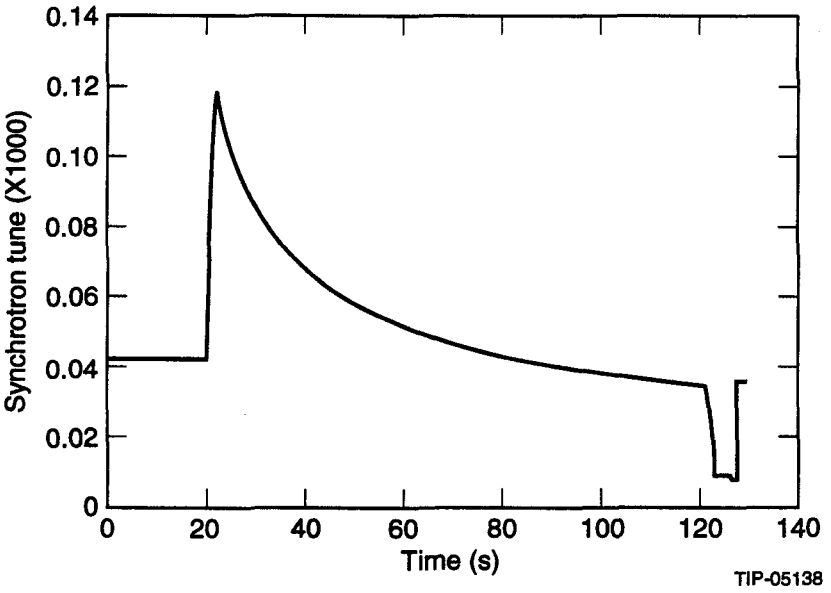

Figure 10. The HEB synchrotron tune cycle.

3.11 The Energy Spread ($\delta E/E_s$) Cycle

Derivation of Formula

Section 3.9 gives the derivation of Eq. (58) for the phase evolution for an arbitrary particle, repeated here as Eq. (61)

$$\delta\phi = A\sin(\omega_s t + \psi)\ , \text{ with } \omega_s = (f_0/\beta)(-2\pi h\eta QV\cos\phi_s/E_s)^{1/2}. \tag{61}$$

Section 3.9 also gives the derivation for the finite difference equation for $\delta\phi$, Eq. (49), repeated here as Eq. (62)

$$d(\delta\phi)/dt = 2\pi h\eta\beta^{-2}f_0(\delta E)/E_s\,. \tag{62}$$

Equation (62) can be rearranged to yield an expression for δE,

$$\delta E = (E_s\beta^2/2\pi h\eta f_0)d(\delta\phi)/dt = (E_s\beta^2/2\pi h\eta f_0)\omega_s A\cos(\omega_s t + \psi). \tag{63}$$

Since $\omega_s = (f_0/\beta)(-2\pi h\eta QV\cos\phi_s/E_s)^{1/2}$, δE can be rewritten as

$$\delta E = (\beta)(-QV\cos\phi_s E_s/2\pi h\eta)^{1/2} A\cos(\omega_s t + \psi). \tag{64}$$

It is desirable at this point to switch variables from energy and phase to energy and time. Recalling that an advance in $\delta\phi$ of 2π radians is equivalent to a time advance of one rf period, $\delta t = \Delta t_{RF}\delta\phi/2\pi = \Delta t_s\delta\phi/2\pi h = \delta\phi/2\pi h f_0 = A\sin(\omega_s t + \psi)/2\pi h f_0$, or

$$\delta t = A\sin(\omega_s t + \psi)/2\pi h f_0 \text{, with } \omega_s = (f_0/\beta)(-2\pi h\eta QV\cos\phi_s/E_s)^{1/2}. \tag{65}$$

If the energy deviation is plotted versus the time deviation, the particle will trace out an ellipse over time. The area within the ellipse is the longitudinal emittance of the particle, ε_{Lp}. The area within the ellipse described by Eqs. (64) and (65) is

$$\varepsilon_{Lp} = \pi\delta E_{max}\delta t_{max}, \tag{66}$$

where δE_{max} and δt_{max} are the maximum values of δt and δE, respectively, obtained by the particle during its trajectory.

Each particle will trace out its own ellipse, and have its own longitudinal emittance. For some value of the emittance, ε_{L95}, 95% of the individual emittances will be less than ε_{L95}, and the trajectories of 95% of the particles will lie within the ε_{L95} ellipse. Here the "beam energy spread," δE_{95}, and "beam temporal spread," δt_{95}, are defined to be the maximum energy deviation and the maximum time deviation of the ε_{L95} ellipse, respectively. For the 95% ellipse:

$$\delta E_{95} = \beta(-QV\cos\phi_s E_s/2\pi h\eta)^{1/2} A_{95}. \tag{67}$$

$$\delta\tau_{95} = A_{95}/2\pi h f_0. \tag{68}$$

The area of the 95% ellipse is $\pi\delta E_{95}\delta\tau_{95}$,

$$\varepsilon_{L95} = \pi\beta(-QV\cos\phi_s E_s/2\pi h\eta)^{1/2} A_{95}^2/2\pi h f_0. \tag{69}$$

Expression (69) can be rearranged to yield an expression for A_{95}:

$$A_{95} = (\varepsilon_{L95} 2\pi h f_0/\beta\pi)^{1/2}(-2\pi h\eta/QV\cos\phi_s E_s)^{1/4}. \tag{70}$$

Equation (70) can now be substituted into (71):

$$\delta E_{95} = (f_0\beta\varepsilon_{L95}/\pi)^{1/2}(-2\pi hQV\cos\phi_s E_s/\eta)^{1/4}. \tag{71}$$

It is usual to express the quantity of interest as $\delta E_{95}/E_s$:

$$\delta E_{95}/E_s = (f_0\beta\varepsilon_{L95}/\pi E_s)^{1/2}(-2\pi hQV\cos\phi_s/E_s\eta)^{1/4}. \tag{72}$$

The quantity of interest for such items as calculation of instabilities is not δE_{95}, but rather one standard deviation of the distribution, σ_E. The area of the ellipse of the particle that has a maximum energy displacement σ_E and a maximum time displacement σ_t is $\pi\sigma_E\sigma_t$, yet for some ungodly reason the quantity ε_L associated with this ellipse has been defined in the SSC literature to be

$$\varepsilon_L = \sigma_E\sigma_t \text{ . (No } \pi\text{!!).} \tag{73}$$

Thus, the emittance of the beam associated with the one sigma quantities is not the area of the phase space defined by an ellipse of axes σ_E and σ_t, but rather that area divided by π. Since the π has already been divided out, the formula for σ_E/E_s becomes

$$\sigma_E/E_s = (f_0\beta\varepsilon_L/E_s)^{1/2}(-2\pi hQV\cos\phi_s/E_s\eta)^{1/4}. \tag{74}$$

Nonetheless, the 95% emittance is defined here and in the SSC literature as the area of the ellipse that surrounds 95% of the particle phase space trajectories, and both this document and the SSC literature assume, for now, that the beam will have a gaussian distribution in longitudinal phase space, hence

$$\varepsilon_{L95} = 6\pi\sigma_E\sigma_t = 6\pi\varepsilon_L, \tag{75}$$

and since the program ELVIRA uses ε_{L95}, it is desirable to express (74) in terms of ε_{L95},

$$\sigma_E/E_s = (f_0\beta\varepsilon_{L95}/6\pi E_s)^{1/2}(-2\pi hQV\cos\phi_s/E_s\eta)^{1/4}. \tag{76}$$

Q and π are physical constants, h is a machine specific constant, f_0 and β are derived in Section 3.6, η is derived in Section 3.9, E_s is derived in Section 3.5, V is either an input discussed in Section 2.6.1 or it is derived from an input bucket area as discussed in Section 3.22, ε_{L95} is an input discussed in Section 2.5 and ϕ_s is derived in Section 3.8.

Location of Coding in elvira.f

The coding for σ_E/E_s is found on the lines labeled 0930 and 0940 in the source code elvira.f, σ_E/E_s is multiplied by 1000 for plotting purposes in line 0950 and the printing is coded into line 0960.

Graphical Representation

Figure 11 depicts the HEB σ_E/E_s cycle.

Discussion

As can be seen from Figure 11 σ_E/E_s starts out at 8.81×10^{-5}, then rises during the first parabolic magnetic ramp to 1.43×10^{-4}, decreases to 3.52×10^{-5} just before the magnetic flat top, decreases to 1.76×10^{-5} during the second parabolic magnet ramp, remains at this level during the final setting of the timing for transfer, decreases to 1.65×10^{-5} during the adiabatic decrease in bucket area, and finally increases to 3.58×10^{-5} just before extraction.

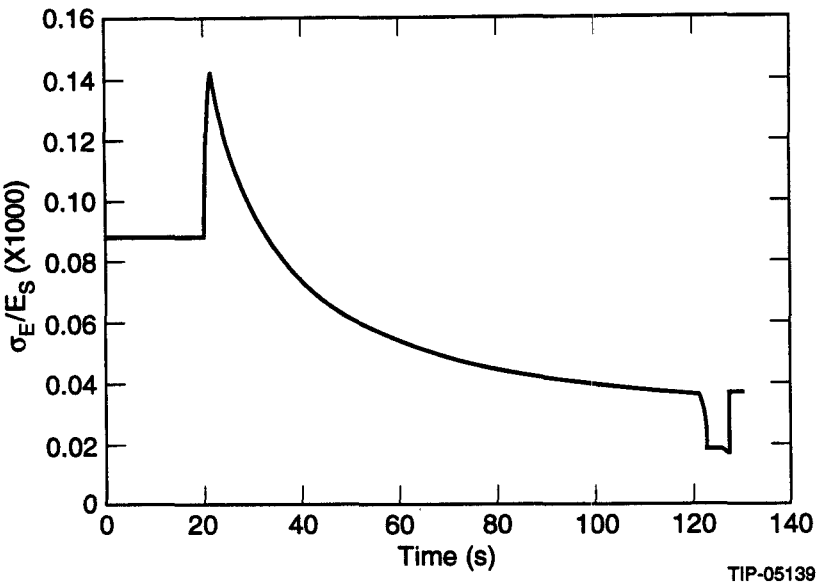

Figure 11. The HEB σ_E/E_s cycle.

3.12 The Momentum Spread ($\delta p/p_s$) Cycle

Derivation of Formula

It is an empirical observation that $E = (p^2c^2 + m^2c^4)^{1/2}$, where E is the particle energy, $E = \gamma mc^2$, p the particle momentum, $p = \beta\gamma mc$, m the (rest) mass of the particle and c the velocity of light. Since m and c are constants, differentiating each side of this relation leaves

$$dE = pc^2dp/E, \tag{77}$$

and thus

$$dE/E = (pc/E)^2(dp/p) = (\beta\gamma mc^2/\gamma mc^2)^2(dp/p) = \beta^2(dp/p). \tag{78}$$

Thus, $dp/p = \beta^{-2}(dE/E)$. Since σ_E/E_s and σ_p/p_s are small numbers a valid approximation is

$$\sigma_p/p_s = \beta^{-2}(\sigma_E/E_s). \tag{79}$$

!APPROXIMATION!

β is defined in Section 3.6 and σ_E/E_s is defined in Section 3.11.

Location of Coding in elvira.f

The coding for σ_p/p_s is found on the line labeled 0970 in the source code elvira.f, σ_p/p_s is multiplied by 1000 for plotting purposes in line 0980 and the printing is coded into line 0990.

Graphical Representation

Figure 12 depicts the HEB σ_p/p_s cycle.

Discussion

As can be seen from Figure 12 σ_p/p_s starts out at 8.81×10^{-5}, then rises during the first parabolic magnetic ramp to 1.43×10^{-4}, decreases to 3.52×10^{-5} just before the magnetic flat top, decreases to 1.76×10^{-5} during the second parabolic magnet ramp, remains at this level during the final setting of the timing for transfer, decreases to 1.65×10^{-5} during the adiabatic decrease in bucket area, and finally increases to 3.58×10^{-5} just before extraction.

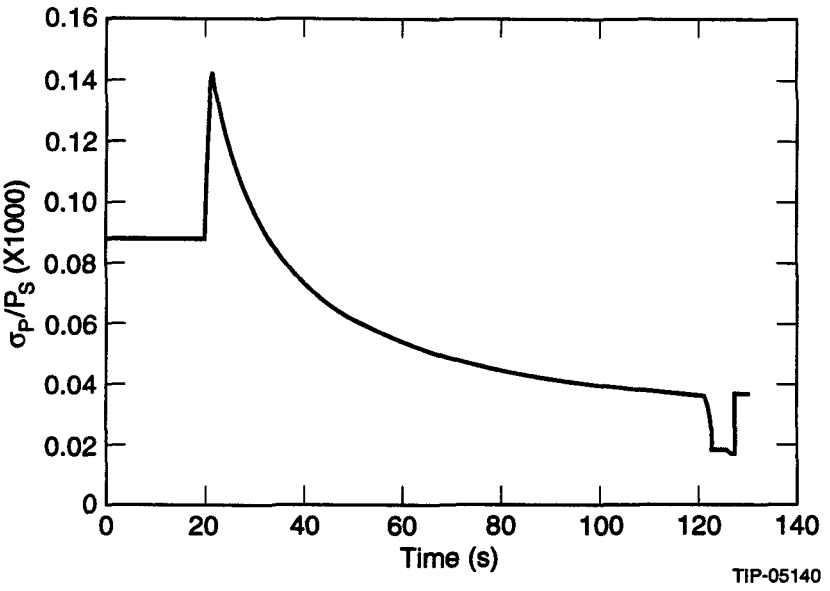

Figure 12. The HEB σ_P/P_s cycle.

3.13 The Temporal Bunch Spread (σt) Cycle

Derivation of Formula

ε_{L95} is defined above in Eq. (75), repeated here as (80),

$$\varepsilon_{L95} = 6\pi\sigma_E\sigma_t \,. \tag{80}$$

Rearranging Eq. (80) leaves

$$\sigma_t = \varepsilon_{L95}/6\pi\sigma_E = \varepsilon_{L95}/[6\pi E_s(\sigma_E/E_s)] \,. \tag{81}$$

ε_{L95} is an input discussed in Section 2.5, π is a physical constant, E_s is defined in Section 3.5 and σ_E/E_s is defined in Section 3.11.

Location of Coding in elvira.f

The coding for σ_t is found on the line labeled 1000 in the source code elvira.f, σ_t is multiplied by 1.E9 for plotting purposes in line 1010 and the printing is coded into line 1020.

Graphical Representation

Figure 13 depicts the HEB σ_t cycle.

Discussion

As can be seen from Figure 13 σ_t starts out at 0.993 ns, then decreases during the first parabolic magnetic ramp to 0.576 ns, decreases to 0.500 ns by the end of the acceleration, increases to 0.993 ns during the second parabolic ramp, remains at this level during the final setting of the timing for transfer, increases to 1.06 ns during the adiabatic decrease in the bucket area, and finally decreases to 0.489 ns just before extraction.

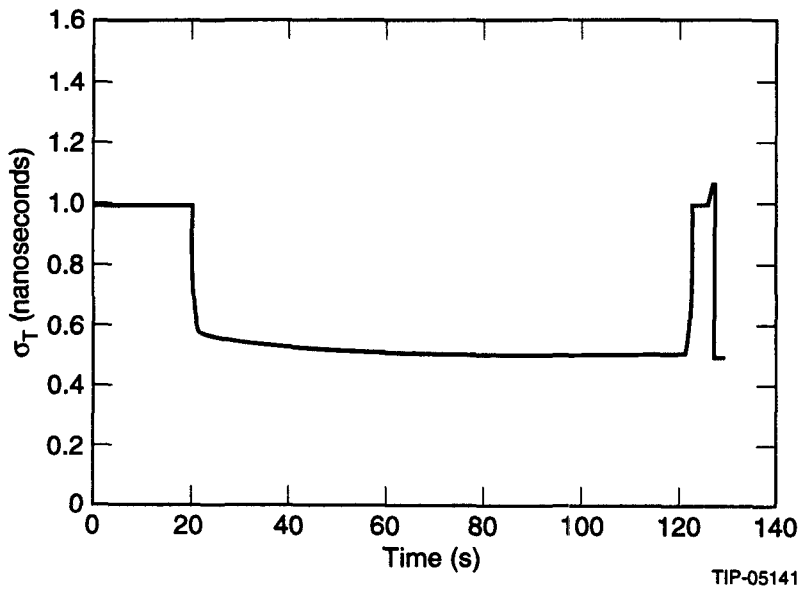

Figure 13. The HEB temporal bunch length (σ_T) cycle.

3.14 The Spatial Bunch Spread (σ_z) Cycle

Derivation of Formula

The velocity of the particles, βc, is defined as the distance traveled by the particles per unit time. Therefore, if the first particle in the bunch passes a given point at a time σ_t earlier than a second particle, it will have travelled a distance

$$\sigma_z = \beta c \sigma_t \tag{82}$$

in that time. If σ_t is the one sigma temporal separation of particles within the bunch, then $\sigma_z = \beta c \sigma_t$ is the one sigma spatial separation of particles within the bunch.

c is a physical constant, β is defined in Section 3.6, and σ_t is defined in Section 3.13.

Location of Coding in elvira.f

The coding for σ_z is found on the line labeled 1030 in the source code elvira.f, σ_s is multiplied by 1000 for plotting purposes in line 1040 and the printing is coded into line 1050.

Graphical Representation

Figure 14 depicts the HEB σ_z cycle.

Discussion

As can be seen from Figure 14 σ_z starts out at 298 mm, then decreases during the first parabolic magnetic ramp to 173 mm, decreases to 150 mm by the end of the acceleration, increases to 298 mm during the second parabolic ramp, remains at this level during the final setting of the timing for transfer, increases to 318 mm during the adiabatic decrease in the bucket area, and finally decreases to 147 mm just before extraction.

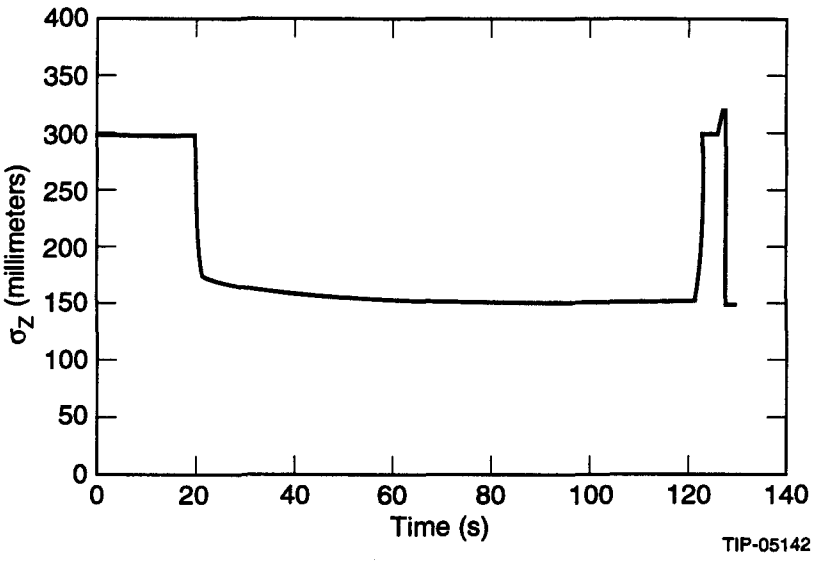

Figure 14. The HEB spatial bunch length (σ_Z) cycle.

3.15 The Relative Energy Half Bucket Height ($\Delta E_B/E_s$) Cycle

Derivation of Formula

Up to this point the concern has been with small oscillations about the synchronous energy and phase. Another important concern is the limit of stability of the oscillations. When the energy and phase are too far from the synchronous values, particles will no longer oscillate about the synchronous values, and they will be lost. This section will calculate the maximum relative energy spread that can be contained in an oscillatory motion.

Section 3.9 derives Eq. (36), which is the differential equation relating the change in δE to the phase of the particle, repeated here as Eq. (83).

$$d(\delta E)/dt = f_0 Q V(\sin\phi - \sin\phi_s). \tag{83}$$

Section 3.9 also derives Eq. (49), which is the formula for $d(\delta\phi)/dt$, repeated here as (84), but with a simplification of notation. Section 3.9 defines $\phi = \phi_s + \delta\phi$, and since $d\phi_s/dt = 0$, $d(\delta\phi)/dt = \delta\phi/dt$ and $d^2(\delta\phi)/dt^2 = d^2\phi/dt^2$.

$$d\phi/dt = 2\pi h\eta\beta^{-2}f_0(\delta E)/E_s. \tag{84}$$

Note that $d\phi_s/dt = 0$ is not always exact, so this is an approximation.

!APPROXIMATION!

The coupled differential equations (83) and (84) can lead to stable oscillations about the synchronous energy and phase only if the initial energy and phase are sufficiently close to the synchronous values. The region of sufficiently close initial values is an area in phase space, and that area is called the bucket area. Calculation of the bucket area will require an evaluation of $d^2\phi/dt^2$. Section 3.9 derives (55), which is the formula for $d^2(\delta\phi)/dt^2$, repeated here as Eq. (85),

$$d^2\phi/dt^2 = (2\pi h\eta f_0^2/E_s\beta^2)QV(\sin\phi - \sin\phi_s). \tag{85}$$

Now multiply both sides of (85) by $d\phi/dt$ and rearrange it to yield,

$$[d^2\phi/dt^2 - (2\pi h\eta f_0^2/E_s\beta^2)QV(\sin\phi - \sin\phi_s)]d\phi/dt = 0. \tag{86}$$

Integrating (86) with respect to time leaves

$$[d\phi/dt]^2/2 + (2\pi h\eta f_0^2/E_s\beta^2)QV(\cos\phi + \phi\sin\phi_s) = K, \tag{87}$$

where K is a constant of the motion (since its derivative with respect to time is zero). The constant K can be evaluated at a single point in the trajectory. Since the interest is a determination of where motion is stable, and since stable oscillations must pass through the synchronous energy, it is desirable to pick a point for evaluation of K that has the synchronous energy, $d\phi/dt = \delta E = 0$.

EVALUATION OF THE SEPARATRIX

The boundary in phase space between the region where stable oscillations take place and the region where motion is unstable is called the separatrix. The equation for the separatrix can be determined by finding the maximum or minimum angle ϕ_2 for which motion is stable. Substituting the extreme value into (87) will then allow a determination of K for the separatrix,

$$K_s = (2\pi h\eta f_0^2/E_s\beta^2)QV(\cos\phi_2 + \phi_2\sin\phi_s) \tag{88}$$

and this in turn allows a determination of the equation of the separatrix. The evolution of ϕ on the separatrix is thus governed by

$$d\phi/dt = \pm\ 1\{(4\pi h\eta f_0^2/E_s\beta^2)QV[(\cos\phi_2 + \phi_2\sin\phi_s) - (\cos\phi + \phi\sin\phi_s)]\}^{1/2}. \tag{89}$$

In general the synchronous phase angle, ϕ_s, can take on any value from $-\pi$ to π. But the above expression possesses sufficient symmetry so that once the separatrix is known for synchronous angles having values

between 0 and $\pi/2$, a simple variable substitution can be made to determine the equation of the separatrix for the remaining cases. Since both the bucket area and the bucket width must be determined numerically, use of these substitutions allows a reduction in the amount of tabular data and a simplification of the formulas used to fit the data. The relations relating the various regions are:

$$\theta = \phi + \pi \text{ (or } \phi = \theta - \pi) \text{ for } -\pi < \phi < -\pi/2 . \tag{90}$$

$$\theta = -\phi \text{ (or } \phi = -\theta) \text{ for } -\pi/2 < \phi < 0 . \tag{91}$$

$$\theta = \phi \text{ (or } \phi = \theta) \text{ for } 0 < \phi < \pi/2 . \tag{92}$$

$$\theta = \pi - \phi \text{ (or } \phi = \theta + \pi) \text{ for } \pi/2 < \phi < \pi . \tag{93}$$

By substituting θ_2, θ_s, and θ, for ϕ_2, ϕ_s, and ϕ, respectively into Eq. (89) leaves

$$d\theta/dt = \pm\ 1\{(4\pi h|\eta|f_0^2/E_s\beta^2)QV[(\cos\theta + \theta\sin\theta_s) - (\cos\theta_2 + \theta_2\sin\theta_s)]\}^{1/2}. \tag{94}$$

The substitution also confines θ_s to takes on values only from 0 to $\pi/2$.

It is not obvious, at least to this author, that the transformations given in Eqs. (90) through (93) transform (89) into (94). Each of the four cases will now be considered.

For $-\pi < \phi < -\pi/2$:

Substitution (90) leaves $\cos\phi_2 = \cos(\theta_2 - \pi) = \cos(\theta_2)\cos(-\pi) - \sin(\theta_2)\sin(-\pi) = -\cos(\theta_2)$; $\phi_2\sin\phi_s = (\theta_2 - \pi)\sin(\theta_s - \pi) = (\theta_2 - \pi)[\sin(\theta_s)\cos(-\pi) + \cos(\theta_s)\sin(-\pi)] = -(\theta_2 - \pi)\sin(\theta_s)$; $\cos\phi = \cos(\theta - \pi) = \cos(\theta)\cos(-\pi) - \sin(\theta)\sin(-\pi) = -\cos(\theta)$; and $\phi\sin\phi_s = (\theta - \pi)\sin(\theta_s - \pi) = (\theta - \pi)[\sin(\theta_s)\cos(-\pi) + \cos(\theta_s)\sin(-\pi)] = -(\theta - \pi)\sin(\theta_s)$. Therefore, what is left to evaluate is $[(\cos\phi_2 + \phi_2\sin\phi_s) - (\cos\phi + \phi\sin\phi_s)] = [-\cos(\theta_2) - (\theta_2 - \pi)\sin(\theta_s) + \cos(\theta) + (\theta - \pi)\sin(\theta_s)] = [-\cos\theta_2 - \theta_2\sin\theta_s + \cos\theta + \theta\sin\theta_s]$. For this range of ϕ a machine is above transition and η is positive, so (94) results from substituting (90) into (89).

For $-\pi/2 < \phi < 0$:

Substitution (91) leaves $\cos\phi_2 = \cos(-\theta_2) = \cos\theta_2$; $\phi_2\sin\phi_s = (-\theta_2)\sin(-\theta_s) = \theta_2\sin\theta_s$; $\cos\phi = \cos(-\theta) = \cos\theta$; and $\phi\sin\phi_s = (-\theta)\sin(-\theta_s) = \theta\sin\theta_s$. Therefore, $[(\cos\phi_2 + \phi_2\sin\phi_s) - (\cos\phi + \phi\sin\phi_s)] = [\cos\theta_2 + \theta_2\sin\theta_s - \cos\theta - \theta\sin\theta_s]$. For this range of ϕ a machine is below transition and η is negative, so forming the absolute value of η requires multiplication by -1, and if this -1 is multiplied by the trig functions (94) clearly results from substituting (91) into (89).

For $0 < \phi < \pi/2$:

Substitution (92) leaves $\cos\phi_2 = \cos\theta_2$; $\phi_2\sin\phi_s = \theta_2\sin\theta_s$; $\cos\phi = \cos\theta$; and $\phi\sin\phi_s = \theta\sin\theta_s$. Therefore, $[(\cos\phi_2 + \phi_2\sin\phi_s) - (\cos\phi + \phi\sin\phi_s)] = [\cos\theta_2 + \theta_2\sin\theta_s - \cos\theta - \theta\sin\theta_s]$. For this range of ϕ a machine is below transition and η is negative, so forming the absolute value of η requires multiplication by -1, and if this -1 is multiplied by the trig functions (94) clearly results from substituting (92) into (89).

For $\pi/2 < \phi < \pi$:

Substitution (93) leaves $\cos\phi_2 = \cos(\pi + \theta_2) = \cos(\pi)\cos(\theta_2) - \sin(\pi)\sin(\theta_2) = -\cos(\theta_2)$; $\phi_2\sin\phi_s = (\pi + \theta_2)\sin(\pi + \theta_s) = (\pi + \theta_2)[\sin(\pi)\cos(\theta_s) + \cos(\pi)\sin(\theta_s)] = -(\pi + \theta_2)\sin(\theta_s)$; $\cos\phi = \cos(\pi + \theta) =$

$\cos(\pi)\cos(\theta) - \sin(\pi)\sin(\theta) = -\cos(\theta)$; and $\phi\sin\phi_s = (\pi + \theta)\sin(\pi + \theta_s) = (\pi + \theta)[\sin(\pi)\cos(\theta_s) + \cos(\pi)\sin(\theta_s)] = -(\pi+\theta)\sin(\theta_s)$. Therefore, $[(\cos\phi_2+\phi_2\sin\phi_s)-(\cos\phi+\phi\sin\phi_s)] = [-\cos(\theta_2)-(\pi+\theta_2)\sin(\theta_s)+\cos(\theta)+(\pi+\theta)\sin(\theta_s)] = [-\cos\theta_2-\theta_2\sin\theta_s+\cos\theta+\theta\sin\theta_s]$. For this range of ϕ a machine is above transition and η is positive, so (94) results from substituting (93) into (89).

Now that it has been shown that (94) is equivalent to (89) when the substitutions (90) through (93) are applied, the problem of finding the equation for the separatrix requires finding the maximum angle, θ_2, for which the motion is stable. The evolution of θ is governed by Eq. (94). A maximum for $\theta(t)$ is found at the point where $d\theta/dt = 0$, defined here as $\theta = \theta_2$. The requirement for stability is that the second derivative, $d^2\theta/dt^2$, evaluated at θ_2, be less than zero, $(2\pi h|\eta|f_0^2/E_s\beta^2)QV(\sin\theta_s - \sin\theta_2) < 0$. When this condition is met θ will return toward θ_s and therefore the motion will be stable. For $\theta_2 = \pi - \theta_s - \delta$, $\sin\theta_2 = \sin(\pi - \theta_s - \delta) = \sin(\pi)\cos(-\theta_s-\delta)+\cos(\pi)\sin(-\theta_s-\delta) = \sin(\theta_s+\delta) = \sin(\theta_s)\cos(\delta)+\cos(\theta_s)\sin(\delta)$, and for small δ this leaves $\sin(\pi - \phi_s - \delta) = \sin(\theta_s) + \delta\cos(\theta_s)$. It has been arranged that $0 < \theta_s < \pi/2$, and thus $\cos(\theta_s)$ is greater than zero. Therefore the quantity $(\sin\theta_s - \sin\theta_2)$ will be less than zero for positive δ. A positive δ therefore leads to $d^2\theta/dt^2 < 0$, and stable motion. Negative δ leads to $d^2\theta/dt^2 > 0$, and unstable motion. Thus, the maximum value of θ for which motion is stable is

$$\theta_2 = \pi - \theta_s. \tag{95}$$

(Note that while the sign of $d^2\theta/dt^2$ indicates stability since θ immediately begins to return toward θ_s, it is possible that the other sign of $d^2\theta/dt^2$ could also be on a stable orbit, if later on in the orbit θ eventually reverses direction, and returns toward θ_s. The proof that this does not happen will not be presented at this time. Thus it has been shown here that the function θ exhibits a local maximum, but the global properties of the function have not been investigated.)

!OMISSION!

The equation for the separatrix is determined by substituting (95) into (94)

$$d\theta/dt = \pm\ 1\{(4\pi h|\eta|f_0^2/E_s\beta^2)QV[(\cos\theta + \theta\sin\theta_s) - (\cos(\pi - \theta_s)+(\pi - \theta_s)\sin\theta_s)]\}^{1/2}. \tag{96}$$

The maximum value of $d\theta/dt$ (as a function of θ) will be found where it's derivative with respect to θ is zero, and this occurs when $\theta = \theta_s$. Therefore, the maximum value of $d\theta/dt$ is

$$(d\theta/dt)_{MAX} = \{(4\pi h|\eta|f_0^2/E_s\beta^2)QV[(\cos\theta_s + \theta_s\sin\theta_s) - (\cos(\pi - \theta_s) + (\pi - \theta_s)\sin\theta_s)]\}^{1/2}$$

$$= \{(4\pi h|\eta|f_0^2/E_s\beta^2)QV[2\theta_s\sin\theta_s + 2\cos\theta_s - \pi\sin\theta_s]\}^{1/2}. \tag{97}$$

Substituting (97) into (84) and rearranging leaves an expression for the maximum value of $(\Delta E_B)/E_s$,

$$(\Delta E_B)/E_s = [(\delta E)/E_s]_{MAX} = \beta\{(QV/\pi h|\eta|E_s)[2\theta_s\sin\theta_s + 2\cos\theta_s - \pi\sin\theta_s]\}^{1/2}. \tag{98}$$

Q and π are physical constants, h is a machine specific constant, β is derived in Section 3.6, η is derived in Section 3.9, E_s is derived in Section 3.5, V is either an input discussed in Section 2.6.1 or it is derived from an input bucket area as is discussed in Section 3.22, and ϕ_s is derived in Section 3.8.

Location of Coding in elvira.f

The coding to convert η into $|\eta|$ is found on the line labeled 0515 in the source code elvira.f, the coding for θ_s is found on lies 1070 through 1100, and the coding for $(\Delta E_B)/E_s$ is found on the lines 1110 and 1120, $(\Delta E_B)/E_s$ is multiplied by 1000 for plotting purposes in line 1130 and the printing is coded into line 1140.

Graphical Representation

Figure 15 depicts the HEB $(\Delta E_B)/E_s$ cycle.

Discussion

As can be seen from Figure 15 $(\Delta E_B)/E_s$ starts out at 4.71×10^{-4}, then increases during the first parabolic magnetic ramp to 7.99×10^{-4}, slowly decreases to 1.98×10^{-4} until just before the magnetic flat top, decreases to 9.42×10^{-5} during the second parabolic ramp, remains at this level during the final setting of the timing for transfer, decreases to 8.24×10^{-5} during the adiabatic decrease of the bucket area, and finally increases to 3.89×10^{-4} just before extraction.

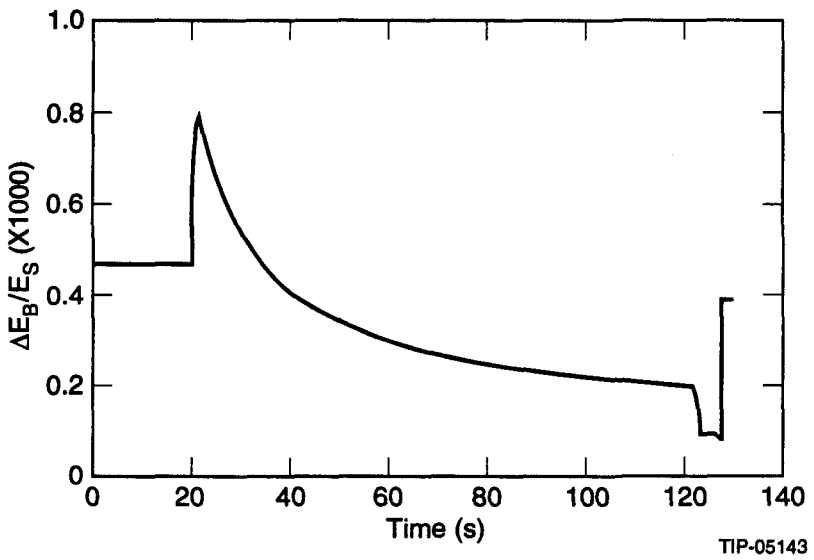

Figure 15. The HEB relative half bucket height $\Delta E_B/E_S$ cycle.

3.16 The Relative Momentum Half Bucket Height $(\Delta p_B/p_s)$ Cycle

Derivation of Formula

Section 3.12 derives the relation $dp/p = \beta^{-2}(dE/E)$. Since $\Delta E_B/E_s$ and $\Delta p_B/p_s$ are small numbers a valid approximation is

$$\Delta p_B/p_s = \beta^{-2}(\Delta E_B/E_s) \,. \tag{99}$$

!APPROXIMATION!

β is defined in Section 3.6, and $\Delta E_B/E_s$ is defined in Section 3.15.

Location of Coding in elvira.f

The coding for $\Delta p_B/p_s$ is found on the line labeled 1150 in the source code elvira.f, $(\Delta p_B)/p_s$ is multiplied by 1000 for plotting purposes in line 1160 and the printing is coded into line 1170.

Graphical Representation

Figure 16 depicts the HEB $(\Delta p_B)/p_s$ cycle.

Discussion

As can be seen from Figure 16 $(\Delta p_B)/p_s$ starts out at 4.71×10^{-4}, then increases during the first parabolic magnetic ramp to 7.99×10^{-4}, slowly decreases to 1.98×10^{-4} until just before the magnetic flat top, decreases to 9.42×10^{-5} during the second parabolic ramp, remains at this level during the final setting of the timing for transfer, decreases to 8.24×10^{-5} during the adiabatic decrease of the bucket area, and finally increases to 3.89×10^{-4} just before extraction.

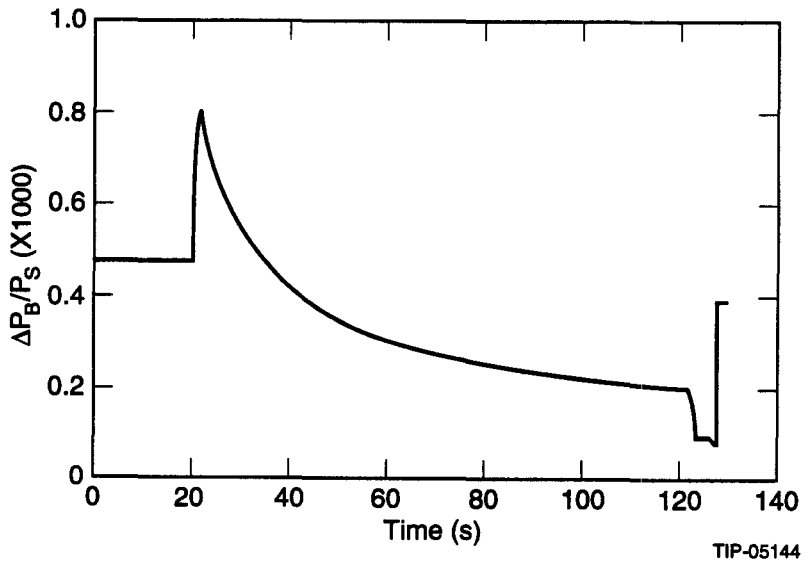

Figure 16. The HEB relative half bucket height $\Delta P_B/P_S$ cycle.

3.17 The Absolute Energy Half Bucket Height (ΔE_B) Cycle

Derivation of Formula

Simple rearrangement leaves

$$\Delta E_B = E_s(\Delta E_B/E_s). \tag{100}$$

E_s is defined in Section 3.5, and $\Delta E_B/E_s$ is defined in Section 3.15.

Location of Coding in elvira.f

The coding for ΔE_B is found on the line labeled 1180 in the source code elvira.f, ΔE_B is converted to GeV for plotting purposes in line 1190 and the printing is coded into line 1200.

Graphical Representation

Figure 17 depicts the HEB ΔE_B cycle.

Discussion

As can be seen from Figure 17 ΔE_B starts out at 0.094 GeV, then increases during the first parabolic magnetic ramp to 0.170 GeV, slowly increases to 0.393 GeV until just before the magnetic flat top, decreases to 0.188 GeV during the second parabolic ramp, remains at this level during the final setting of the timing for transfer, decreases to 0.165 GeV during the adiabatic decrease of the bucket area, and finally increases to 0.777 GeV just before extraction.

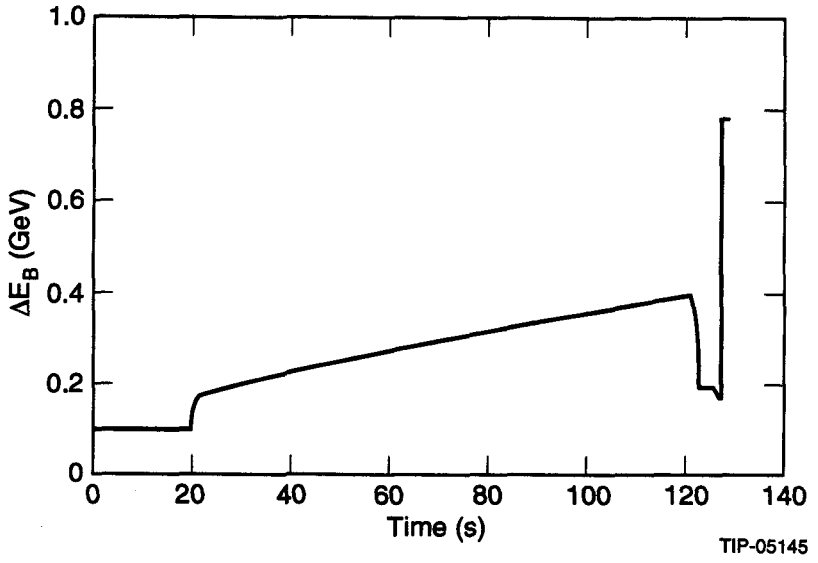

Figure 17. The HEB half bucket energy height (ΔE_B) cycle.

3.18 The Absolute Momentum Half Bucket Height (Δp_B) Cycle

Derivation of Formula

Simple rearrangement leaves

$$\Delta p_B = p_s(\Delta p_B/p_s). \tag{101}$$

p_s is defined in Section 3.4, and $\Delta p_B/p_s$ is defined in Section 3.16.

Location of Coding in elvira.f

The coding for Δp_B is found on the line labeled 1210 in the source code elvira.f, Δp_B is converted to GeV/c for plotting purposes in line 1220 and the printing is coded into line 1230.

Graphical Representation

Figure 18 depicts the HEB Δp_B cycle.

Discussion

As can be seen from Figure 18 Δp_B starts out at 0.094 GeV/c, then increases during the first parabolic magnetic ramp to 0.170 GeV/c, slowly increases to 0.393 GeV/c until just before the magnetic flat top, decreases to 0.188 GeV/c during the second parabolic ramp, remains at this level during the final setting of the timing for transfer, decreases to 0.165 GeV/c during the adiabatic decrease of the bucket area, and finally increases to 0.777 GeV/c just before extraction.

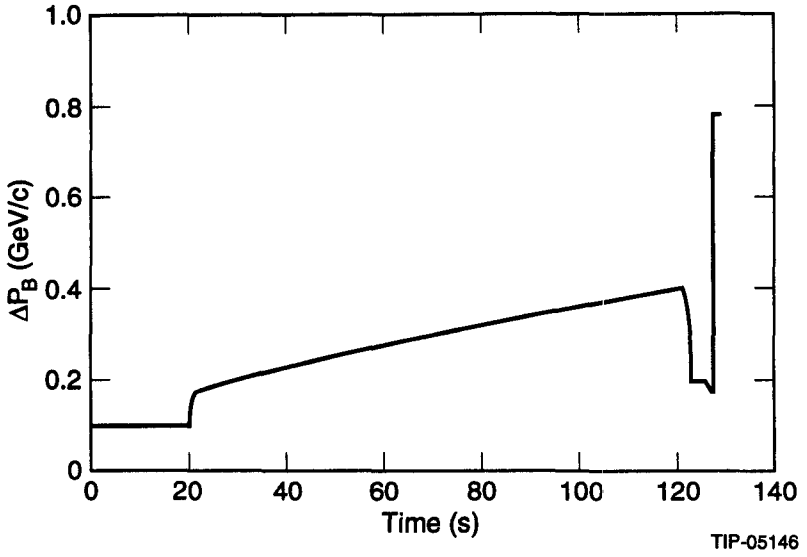

Figure 18. The HEB half bucket momentum height (ΔP_B) cycle.

3.19 The Full Bucket Phase Width ($\Delta\theta_B$) Cycle

Derivation of Formula

Section 3.15 derives the equation for the separatrix, Eq. (96) repeated here as Eq. (102),

$$d\theta/dt = \pm\ 1\{(4\pi h|\eta|f_0^2/E_s\beta^2)QV[(\cos\theta + \theta\sin\theta_s) - (\cos(\pi - \theta_s) + (\pi - \theta_s)\sin\theta_s)]\}^{1/2}. \quad (102)$$

As discussed in Section 3.15, the separatrix is the boundary between stable and unstable longitudinal oscillations. The area of stable oscillations is called the bucket. The bucket phase width is thus equal to the phase separation between the two phases where $d\theta/dt = 0$ on the separatrix. One of the zeros of $d\theta/dt$ on the separatrix is derived in Section 3.15 to be

$$\theta_2 = \pi - \theta_s. \quad (103)$$

The other phase where $d\theta/dt = 0$ is found by solving

$$(\cos\theta_1 + \theta_1\sin\theta_s) - (\cos(\pi - \theta_s) + (\pi - \theta_s)\sin\theta_s) = 0. \tag{104}$$

Equation (104) has been solved numerically, and S. Ohnuma has published formulas that fit the data.[1] For θ_s and θ_1 in degrees these formulas are:

$$\theta_1 = (\theta_s)^{1/2}[25.809 - 3.351\sin\theta_s + 7.050\sin^2\theta_s] - 180 \text{ for } 0 < \sin\theta_s < 0.45, \tag{105}$$

$$\theta_1 = (\theta_s)^{1/2}[25.761 - 1.784\sin\theta_s + 3.717\sin^2\theta_s] - 180 \text{ for } 0.45 < \sin\theta_s < 0.9, \tag{106}$$

$$\theta_1 = 2\theta_s[1 - 0.0657\sin\theta_s + 0.0677\sin^2\theta_s] - 90 \text{ for } 0.9 < \sin\theta_s < 1.0. \tag{107}$$

!APPROXIMATION!

(The formulas just stated are not derived here. ELVIRA does not have a routine dedicated to finding θ_1. Another code would be needed to generate θ_1, and then a fitting of the numerical data to the curves would be required if one wants a complete derivation.)

!OMISSION!

The bucket width is then

$$\Delta\theta_B = \theta_2 - \theta_1 . \tag{108}$$

Location of Coding in elvira.f

The coding for $\Delta\theta_B$ is found on the lines labeled 1240 through 1340 in the source code elvira.f. Printing is coded into line 1350.

Graphical Representation

Figure 19 depicts the HEB $\Delta\theta_B$ cycle.

Discussion

As can be seen from Figure 19 $\Delta\theta_B$ starts out at $2\pi = 6.28$, then decreases during the first parabolic magnetic ramp to 3.18, decreases to 2.76 just before the magnetic flat top, increases to 6.28 at the start of the flat top and remains there until extraction.

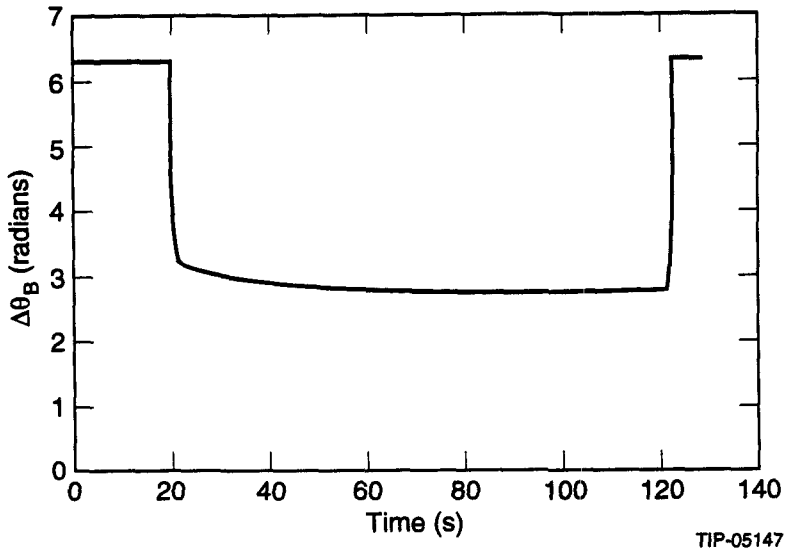

Figure 19. The HEB full bucket phase width ($\Delta\theta_B$) cycle.

3.20 The Full Bucket Temporal Width (Δt_B) Cycle

Derivation of Formula

The rf voltage will undergo a full cycle during one rf period. Hence, for one period of a non-accelerating bucket, $\Delta t_B = 1/f_{RF}$ and $\Delta\theta_B = 2\pi$. In general, the phase width of the rf bucket varies linearly with time width so the expression relating the two is:

$$\Delta t_B = \Delta\theta_B / 2\pi f_{RF} . \tag{109}$$

π is a physical constant, f_{RF} is derived in Section 3.6, and $\Delta\theta_B$ is derived in Section 3.19.

Location of Coding in elvira.f

The coding for Δt_B is found on the line labeled 1360 in the source code elvira.f, Δt_B is multiplied by 1.E9 for plotting purposes in line 1370 and the printing is coded into line 1380.

Graphical Representation

Figure 20 depicts the HEB Δt_B cycle.

Discussion

As can be seen from Figure 20 Δt_B starts out at 16.7 ns, then decreases during the first parabolic magnetic ramp to 8.44 ns, decreases to 7.33 ns just before the magnetic flat top, increases to 16.7 ns at the start of the flat top and remains there until extraction.

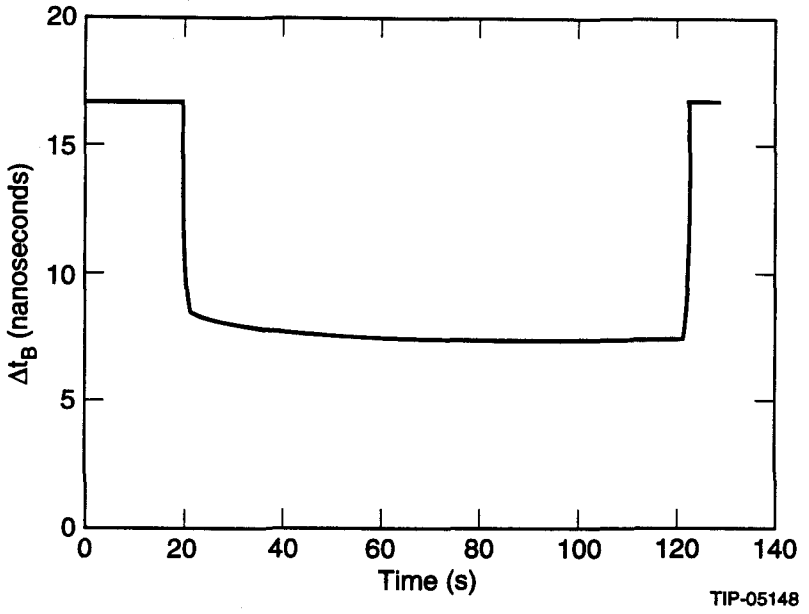

Figure 20. The HEB full bucket temporal width (Δt_B) cycle.

3.21 The Full Bucket Spatial Width (Δz_B) Cycle

Derivation of Formula

The velocity of the particles, βc, is defined as the distance traveled by the particles per unit time. Therefore, if an imaginary first particle passes a given point at a time Δt_B earlier than an imaginary second particle, it will have travelled a distance

$$\Delta z_B = \beta c \Delta t_B \tag{110}$$

in that time, and since Δt_B corresponds to the full bucket temporal width, Δz_B corresponds to the full bucket spatial width.

c is a physical constant, β is defined in Section 3.6, and Δt_B is defined in Section 3.20.

Location of Coding in elvira.f

The coding for Δz_B is found on the line labeled 1390 in the source code elvira.f and the printing is coded into line 1410.

Graphical Representation

Figure 21 depicts the HEB Δz_B cycle.

Discussion

As can be seen from Figure 21 Δz_B starts out at 5.0 meters, then decreases during the first parabolic magnetic ramp to 2.53 meters, decreases to 2.20 meters just before the magnetic flat top, increases to 5.0 meters at the start of the flat top and remains there until extraction.

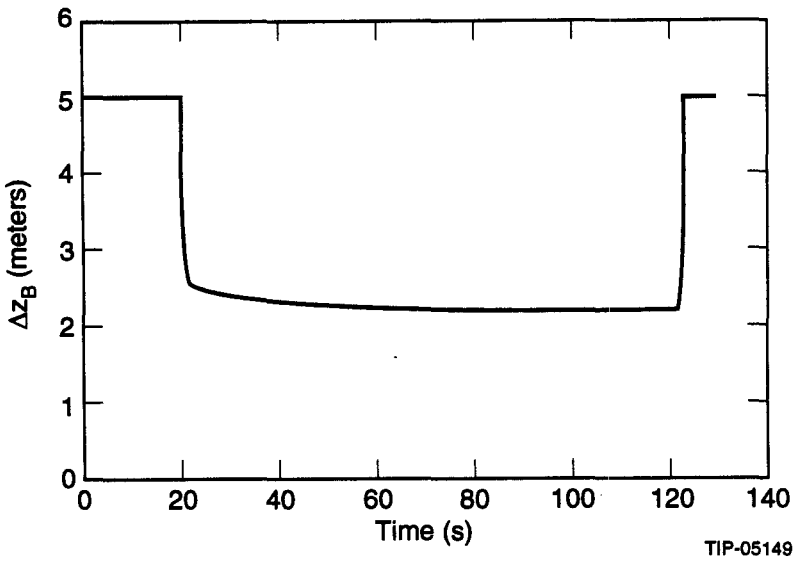

Figure 21. The HEB full bucket spatial length (ΔZ_B) cycle.

3.22 The Bucket Area Cycle

Derivation of Formula

The equation for the separatrix is derived above in Section 3.15, Eq. (96) repeated here as (111).

$$d\theta/dt = \pm\ 1\{(4\pi h|\eta|f_0^2/E_s\beta^2)QV[(\cos\theta + \theta\sin\theta_s) - (\cos(\pi - \theta_s) + (\pi - \theta_s)\sin\theta_s)]\}^{1/2}. \quad (111)$$

The angle θ is defined in Section 3.15, Eqs. (90) through (93), repeated here as Eqs. (112) through (115).

$$\theta = \phi + \pi \text{ (or } \phi = \theta - \pi) \text{ for } -\pi < \phi < -\pi/2. \quad (112)$$

$$\theta = -\phi \text{ (or } \phi = -\theta) \text{ for } -\pi/2 < \phi < 0. \quad (113)$$

$$\theta = \phi \text{ (or } \phi = \theta) \text{ for } 0 < \phi < \pi/2. \quad (114)$$

$$\theta = \pi - \phi \text{ (or } \phi = \theta + \pi) \text{ for } \pi/2 < \phi < \pi. \quad (115)$$

With these definitions it is clear that $d\theta/dt = \pm\ 1d\phi/dt$. Section 3.9 derives Eq. (49), re-expressed in Section 3.15 as (84) and repeated here as (116).

$$d\phi/dt = 2\pi h\eta\beta^{-2}f_0(\delta E)/E_s. \quad (116)$$

Hence,

$$\delta E = (E_s/2\pi h\eta\beta^{-2}f_0)(d\phi/dt) = \pm\ 1(E_s/2\pi h\eta\beta^{-2}f_0)(d\theta/dt)$$

$$= \pm\ 1\{(E_s\beta^2/|\eta|\pi h)QV[(\cos\theta + \theta\sin\theta_s) - (\cos(\pi - \theta_s) + (\pi - \theta_s)\sin\theta_s)]\}^{1/2}. \quad (117)$$

Plotted in δE-θ phase space, the above relation will form two curves, one for the +1 of the ± 1, one for the -1 of the ± 1. As discussed above in Section 3.19, these two curves join each other at the angles θ_1 and θ_2, where θ_2 is derived in Section 3.15 as $\theta_2 = \pi - \theta_s$, and θ_1 is determined numerically. The area bounded by the two curves will be twice the integral of the upper curve, integrated over θ from $\theta = \theta_1$ to $\theta = \theta_2$:

$$A = 2\int_{\theta_2}^{\theta_1} (d\theta)\{(E_s\beta^2/|\eta|\pi h)QV[(\cos\theta + \theta\sin\theta_s) - (\cos(\pi - \theta_s) + (\pi - \theta_s)\sin\theta_s)]\}^{1/2}. \tag{118}$$

It is usual to express the bucket area in terms of a "moving bucket parameter" multiplied by the area of a bucket for which there is no acceleration,

$$A = \alpha(\Gamma)A_0\,, \text{ where } \Gamma = \sin\theta_s\,. \tag{119}$$

The non-accelerating bucket thus corresponds to the case where $\theta_s = 0$, or,

$$A_0 = 2(QVE_s\beta^2/|\eta|\pi h)^{1/2}\int_{\theta_2}^{\theta_1} (d\theta)[\cos\theta + 1]^{1/2}. \tag{120}$$

For $\theta_s = 0$, $\theta_2 = \pi - \theta_s = \pi$. Section 3.19 derives (104), an expression which defines θ_1, repeated here as (121).

$$(\cos\theta_1 + \theta_1\sin\theta_s) - (\cos(\pi - \theta_s) + (\pi - \theta_s)\sin\theta_s) = 0\,. \tag{121}$$

For $\theta_s = 0$, this reduces to $\cos\theta_1 = \cos\pi$, which is satisfied for $\theta_1 = (2n + 1)\pi$, where n is any integer. Since δE is maximum at $\theta_s = 0$, and δE has one zero at $\theta_2 = \pi$, the next time δE passes through 0 as θ decreases from π is at $\theta_1 = -\pi$. By noting that the integrand is an even function,

$$A_0 = 4(QVE_s\beta^2/|\eta|\pi h)^{1/2}\int_{0}^{\pi} (d\theta)[\cos\theta + 1]^{1/2}. \tag{122}$$

Now (by checking the integral tables)

$$\int_{0}^{\pi} (d\theta)[\cos\theta + 1]^{1/2} = 2^{3/2}, \tag{123}$$

so,

$$A_0 = 8\beta(2QVE_s/|\eta|\pi h)^{1/2} \text{ (in units of Joule-radians).} \tag{124}$$

Realizing that an advance of 2π radians is equal to an advance of $1/f_{RF}$ seconds,

$$A_0 = (\beta/\pi f_{RF})\{32E_sQV/|\eta|\pi h\}^{1/2} \text{ (in units of Joule-seconds).} \tag{125}$$

And so in general,

$$A = \alpha(\Gamma)A_0 = \alpha(\Gamma)(\beta/\pi f_{RF})\{32E_sQV/|\eta|\pi h\}^{1/2} \text{ (in units of Joule-seconds)} . \tag{126}$$

It is now possible to define $\alpha(\Gamma)$,

$$\alpha(\Gamma) = A/A_0, \text{ where } \Gamma = \sin\theta_s. \tag{127}$$

In the above expression, A is determined from (118) and A_0 is determined in Eq. (124) (so that both expressions use Joule-radians). It is clear that Eq. (118) is a complicated integral, and for that matter, its lower limit has not been analytically determined here. The integral, along with its lower limit, is usually evaluated numerically, and this document will not derive $\alpha(\Gamma)$ any further, but rather note that the numerical solution of $\alpha(\Gamma)$ was done by F. T. Cole and P. L. Morton,[2] and that it appears in tables. The tabular data has been approximated by formulas.

!OMISSION!

A fit to a seventh order polynomial was completed at Fermilab,[3] and Jim Griffin[4] has shown that $\alpha(\Gamma)$ is closely approximated by

$$\alpha(\Gamma) \sim (1 - \Gamma^{0.79})^{1.27}, (\Gamma = \sin\theta_s). \tag{128}$$

!APPROXIMATION!

IF THE BUCKET AREA IS USED AS AN INPUT

As discussed in Section 2.6, ELVIRA can accept either the rf voltage cycle or the bucket area cycle as an arbitrary input. For the case where the bucket area is used as an arbitrary input, V is a variable that must be solved for, but $V\sin\theta_s = V\Gamma$ is known, since this is the energy gain per turn which is determined by the magnet cycle as discussed in Section 3.7. Substituting (128) into (126) and multiplying by Γ/Γ within the radical leaves

$$A = (1 - \Gamma^{0.79})^{1.27}(\beta/\pi f_{RF})\{32E_sQV\Gamma/|\eta|\pi h\Gamma\}^{1/2} , \tag{129}$$

which can be rearranged as

if $\Gamma > 0$,

$$\{|\eta|\pi h/32E_sQV\Gamma\}^{1/2}(\pi f_{RF}/\beta)A = \Gamma^{-1/2}(1 - \Gamma^{0.79})^{1.27}. \tag{130}$$

An approximate value of Γ can be obtained from the above expression by calculating the left hand side, initializing a trial value of Γ to a small incremental value, and iteratively incrementing Γ by the small incremental amount until the left hand side just exceeds the right hand side. When this happens, a close approximation to Γ has been found.

!APPROXIMATION!

Once Γ is known V is determined by simply dividing $V\Gamma$ by Γ.

$$V = V\Gamma/\Gamma. \tag{131}$$

This procedure only works if Γ is non-zero. For a non-accelerating situation, the voltage can be obtained simply by rearranging (125),

if $\Gamma = 0$,

$$V = (A_0\pi f_{RF}/\beta)^2\{|\eta|\pi h/32E_sQ\}. \tag{132}$$

IF THE VOLTAGE IS USED AS AN INPUT

Finally if the voltage is used as an input, (126) is used to find A,

$$A = \alpha(\Gamma)A_0 = \alpha(\Gamma)(\beta/\pi f_{RF})\{32E_sQV/|\eta|\pi h\}^{1/2} \text{ (in units of Joule-seconds).} \tag{133}$$

Q and π are physical constants, h is a machine specific constant, β is derived in Section 3.6, η is derived in Section 3.9, E_s is derived in Section 3.5, f_{RF} is derived in Section 3.6, either V or A is an input discussed in Section 2.6, $\Gamma = \sin\theta_s$, θ_s is related to ϕ_s as discussed in Section 3.15, and ϕ_s is derived in Section 3.8.

Location of Coding in elvira.f

The voltage and bucket area calculations are found on the lines labeled 0520 through 0810 in the source code elvira.f.

For the case where the bucket area is used as an arbitrary input. For a negligible (or zero) accelerating (or decelerating) voltage, the coding for the voltage is found on lines 0540 through 0570. For a non-negligible accelerating (or decelerating) voltage, the coding for the voltage is found on lines 0580 through 0660. $\alpha(\Gamma)$ is calculated on line 0555 for the case of negligible acceleration (or deceleration) or it is calculated on line 0670 for finite values of acceleration. Printing of $\alpha(\Gamma)$ is coded into line 0680. The voltage is changed to megavolts for printing purposes on line 0690 and printing of the voltage is coded into line 0700.

For the case where the rf voltage is used as an arbitrary input the bucket area is calculated on lines 0720 through 0770. Lines 0720 through 0760 calculate $\alpha(\Gamma)$, the bucket area is calculated on line 0770, the bucket area is converted into eV-seconds for printing purposes on line 0780, the printing of the bucket area is coded into line 0790, and the printing of $\alpha(\Gamma)$ is coded into line 0800.

Graphical Representation

Figure 22 depicts the HEB bucket area cycle.

Discussion

As can be seen from Figure 22 the bucket area starts out at 2.0 eV-seconds, then increases during the magnetic ramp to 4.0 eV-seconds, remains at 4.0 eV-seconds until the bunch rotation is to take place, decreases adiabatically to 3.5 eV-seconds to enable bunch rotation, remains at 3.5 eV-seconds for a final setting of timing for transfer, then suddenly increases to 16.5 eV-seconds to begin the bunch rotation and remains there until extraction.

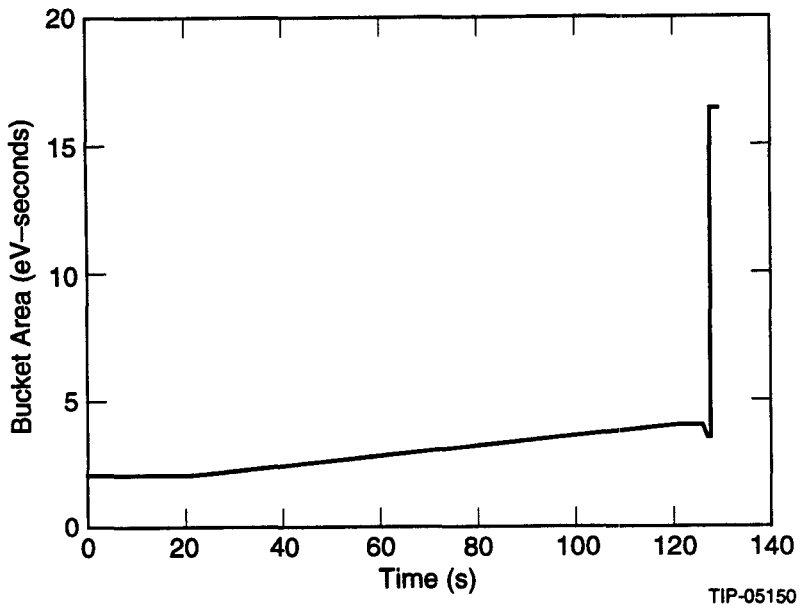

Figure 22. The HEB bucket area cycle.

3.23 The $\alpha(\Gamma)$ Cycle

Derivation of Formula

Since $\alpha(\Gamma)$ is closely tied to the bucket area, the derivation of the formula for $\alpha(\Gamma)$ is discussed above in Section 3.22.

Location of Coding in elvira.f

Since $\alpha(\Gamma)$ is closely tied to the bucket area, the discussion of the coding for $\alpha(\Gamma)$ is discussed above in Section 3.22.

Graphical Representation

Figure 23 depicts the HEB $\alpha(\Gamma)$ cycle.

Discussion

As can be seen from Figure 23 $\alpha(\Gamma)$ starts out at 1, decreases to 0.31 during the first parabolic magnet ramp, decreases to 0.22 during the linear potion of the magnet ramp, increases back to 1 during the second parabolic magnet ramp, and remains at 1 until ejection.

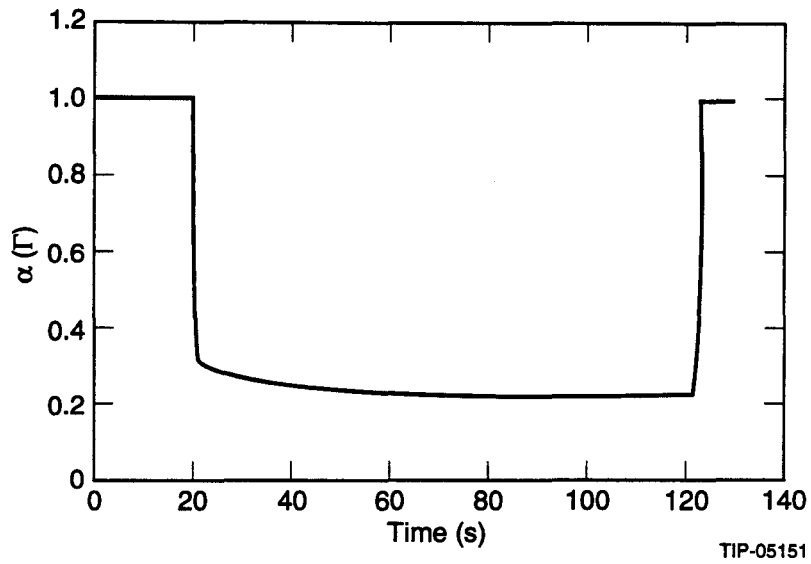

Figure 23. The HEB α(Γ) cycle.

3.24 The Bucket Area Adiabaticity Cycle

Derivation of Formula

The adiabaticity is defined here as the time rate of change of the bucket area multiplied by the synchrotron period and divided by the bucket area,

$$\text{Adiabaticity} = (dA/dt)(1/f_s A), \tag{134}$$

dA is determined as the difference in A during one step through the program, dt is an input to the program, A is defined in Section 3.22 and f_s is defined in Section 3.9.

Location of Coding in elvira.f

The coding for the adiabaticity cycle is found on the lines labeled 1420 through 1490 in the source code elvira.f, with printing coded into line 1480.

Graphical Representation

Figure 24 depicts the HEB adiabaticity cycle.

Discussion

As can be seen from Figure 24 the adiabaticity is essentially zero except for the where the voltage is manipulated to enable the bunch rotation. During the adiabatic decrease in bucket area required to enable bunch rotation the adiabaticity never exceeds 0.07. The sudden increase in voltage required to begin the bunch rotation is, of course, highly non-adiabatic, as shown.

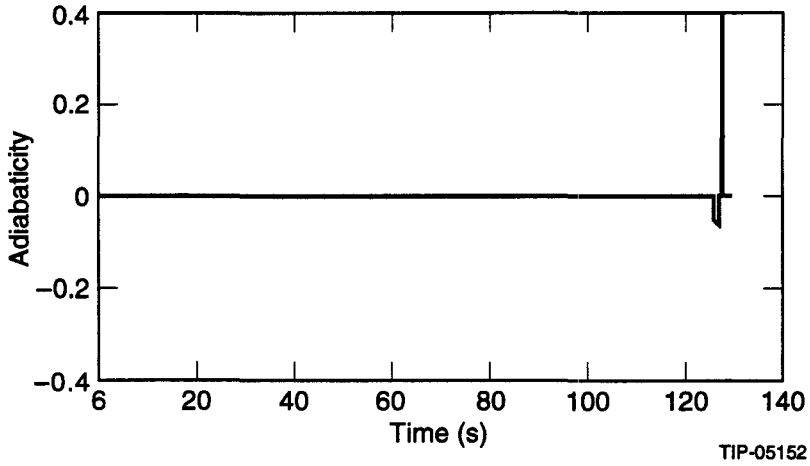

Figure 24. The HEB adiabaticity cycle.

3.24.1 The Bunching Factor Cycle

Derivation of Formula

The bunching factor is defined here as the peak current within the bunch divided by the average current within one bucket-to-bucket spacing.

$$\text{Bunching Factor} = I_{\text{PEAK}}/I_{\text{AVEBKT}} \,. \tag{135}$$

The average current in the bucket is equal to the number of particles in the bunch, N, times the charge per particle, Q, times the velocity of the particles, βc, divided by the bucket to bucket separation, $\beta c/f_{\text{RF}}$, and since the factors of βc cancel out,

$$I_{\text{AVEBKT}} = NQf_{\text{RF}} \,. \tag{136}$$

(Note that the average current within the bucket to bucket spacing is equal to the average current in the storage ring multiplied by the total number of buckets in the ring [the harmonic number] divided by the number of occupied buckets.)

The peak current in the bunch is equal to the peak value of the line density $(dN/dz)_{\text{PEAK}}$ times the charge per particle, Q, times the velocity of the particles βc,

$$I_{\text{PEAK}} = (dN/dz)_{\text{PEAK}} Q\beta c \,. \tag{137}$$

The work here, as well as the present state of SSC literature, assumes a gaussian distribution for the line charge,

$$dN/dz = A\exp(-z^2/2\sigma_z^2). \tag{138}$$

Therefore the total number of particles in the bunch is

$$N = 2\int_0^\infty (dz)\, A\exp(-z^2/2\sigma_z^2) = A(2\pi)^{1/2}\sigma_z\,, \tag{139}$$

where the last equality is obtained by looking up the integral in a table. By inspection of Eq. (138) it is clear that the maximum value of dN/dz is A, and using (139)

$$(dN/dz)_{\mathrm{PEAK}} = A = N/(2\pi)^{1/2}\sigma_z\,. \tag{140}$$

Combining (140), (135), (136), and (137)

$$\text{Bunching Factor} = I_{\mathrm{PEAK}}/I_{\mathrm{AVEBKT}} = (dN/dz)_{\mathrm{PEAK}}Q\beta c/NQf_{\mathrm{RF}} = \beta c/f_{\mathrm{RF}}(2\pi)^{1/2}\sigma_z\,. \tag{141}$$

c and π are physical constants, β and f_{RF} are derived in Section 3.6 and σ_z is derived in Section 3.14.

Location of Coding in elvira.f

The coding for the bunching factor cycle is found on the line labeled 1500 with printing coded into line 1510.

Graphical Representation

Figure 25 depicts the HEB bunching factor cycle.

Discussion

As can be seen from Figure 25 the bunching factor starts out at 6.70, increases to 11.6 during the first parabolic magnet ramp, increases to 13.3 during the acceleration cycle, decreases to 6.70 during the second parabolic ramp, decreases to 6.27 during the adiabatic decrease in bucket area, and finally increases to 13.6 during the voltage step used to initiate bunch rotation, and remains at 13.6 until ejection.

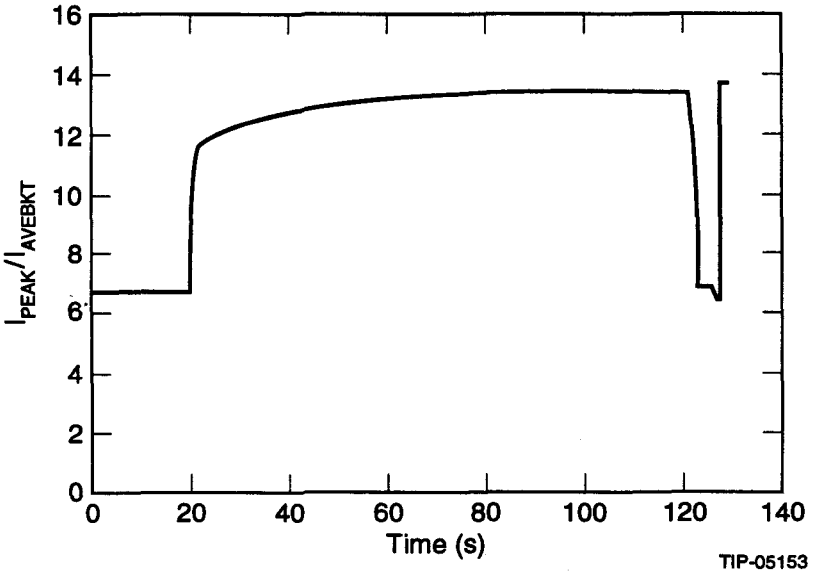

Figure 25. The HEB bunching factor ($I_{\mathrm{PEAK}}/I_{\mathrm{AVEBKT}}$) cycle.

4.0 REFERENCES AND ACKNOWLEDGMENTS

I would like to thank Xiao-Qing Wang and Jay Jayakumar for helpful comments that improved this work.

The original studies of the longitudinal variables of the HEB were done by Miguel Furmann, using his code RAMPRF. RAMPRF results were compared with ELVIRA results to cross check the correctness of the two codes.

This work contains derivations of all the formulae relevant to longitudinal phase space dynamics in particle accelerators. The derivations highlight the presence of approximations and omissions, so that accuracy checking should be possible in every application. The derivations were done independent of any other work, so as to yield a coherent approach. The formulae have all been derived before, perhaps differently, yet reference is not made to the original discovery of the formula. While it is the duty of active science to properly credit the work of others, it is usual to leave this task to textbooks once a field becomes mature, and that is the approach of this note.

References directly referred to in this note are used to fill in the omissions within the note:

1. S. Ohnuma, "The Beam and the Bucket," Fermilab note TM-1381 (1986).
2. F.T. Cole and P.L. Morton, "Areas and Bunching Factors of Partially Filled Buckets," UC Lawrence Radiation Lab Note, UCID 10130/AS/Theoretical/02 (1964).
3. A seventh order fit to $\alpha(\Gamma)$ was obtained from the Fermilab control codes. Fits to $\alpha(\Gamma)$ have been done at FNAL by numerous people, including J.A. Maclachlan, R.P. Johnson and J.P. Marriner, but it is not clear who authored the specific version used in ELVIRA.
4. J. Griffin, private communication.

Collections of longitudinal phase space formulas were used to verify the correctness of the formulas:

5. J.M. Peterson, "RF and Longitudinal-Phase-Space Parameters in the SSC," SSC Note SSC-N-156 (1986).
6. J. Peterson and W. Chou, "SSC Accelerator Physics Formulae," no note number as of my knowledge, March 18, 1991.
7. C. Bovet, *et al.*, "A Selection of Formulae and Data Useful for the Design of A. G. Synchrotrons," CERN Note, CERN/MPS-SI/Int. DL/70/4 (1970).

A well referenced textbook on accelerator physics is:

8. Henri Bruck, "Accelerateurs Circulaires de Particules", Institut National des Sciences et Techniques Nucleaires, Saclay, translated into English as Los Alamos document LA-TR-72-10.

APPENDIX A

In a meeting held on April 30, 1992 between the MEB, HEB and Collider rf and group leaders it was agreed that the HEB should design around an assumption that the MEB will deliver a beam with longitudinal emittance in the range between 0.1 and 0.33 eV-seconds, and that the HEB should deliver a beam to the collider with a longitudinal emittance of 0.66 eV-seconds.

This main body of this work has presented the case where the HEB longitudinal emittance cycle varies between 0.33 and 0.66 eV-seconds.

This appendix will present the graphs (Figures A-1 through A-25) for all of the longitudinal variables for the case where the HEB longitudinal emittance varies between 0.1 and 0.66 eV-seconds.

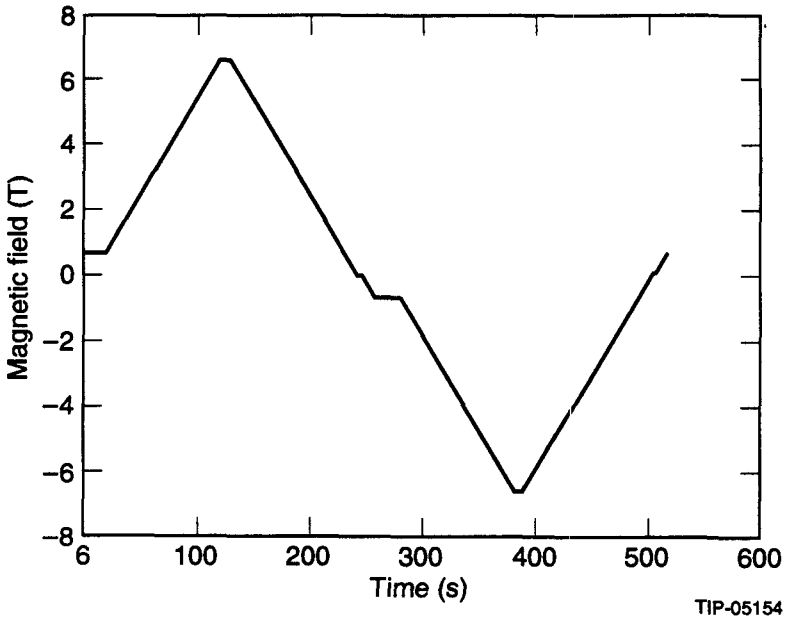

Figure A-1. The HEB magnetic field cycle.

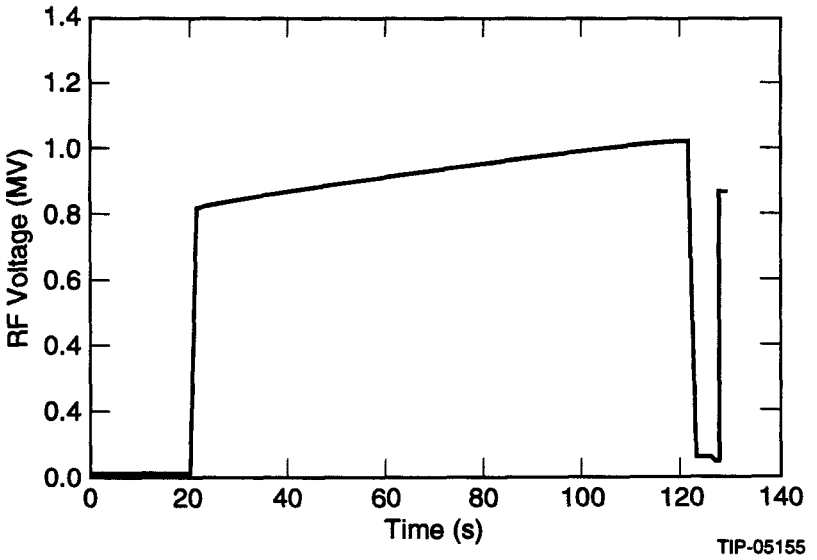

Figure A-2. The HEB rf voltage cycle.

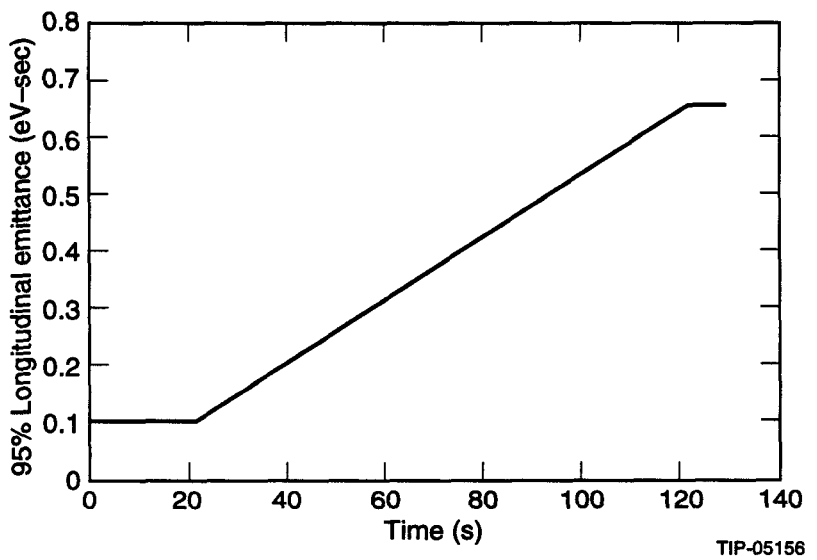

Figure A-3. The HEB 95% longitudinal emittance cycle.

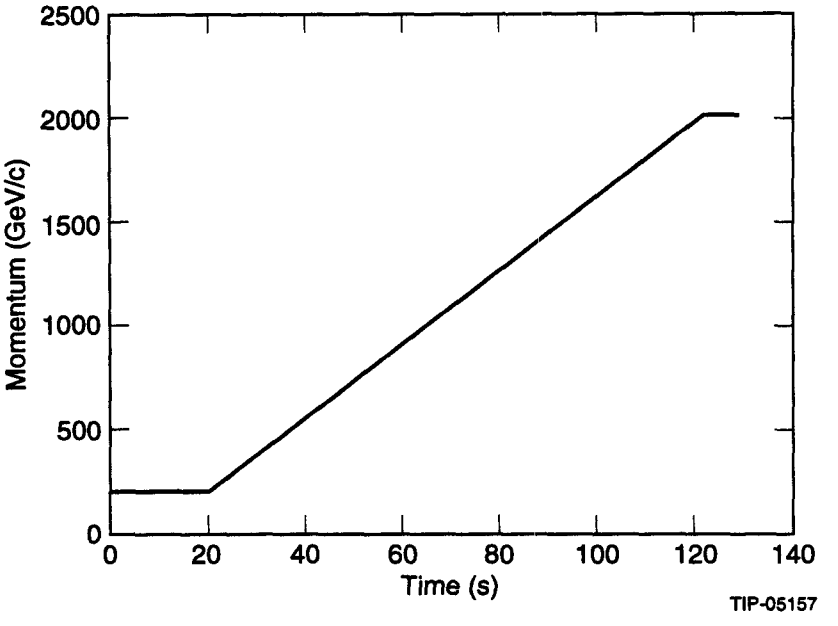

Figure A-4. The HEB momentum cycle.

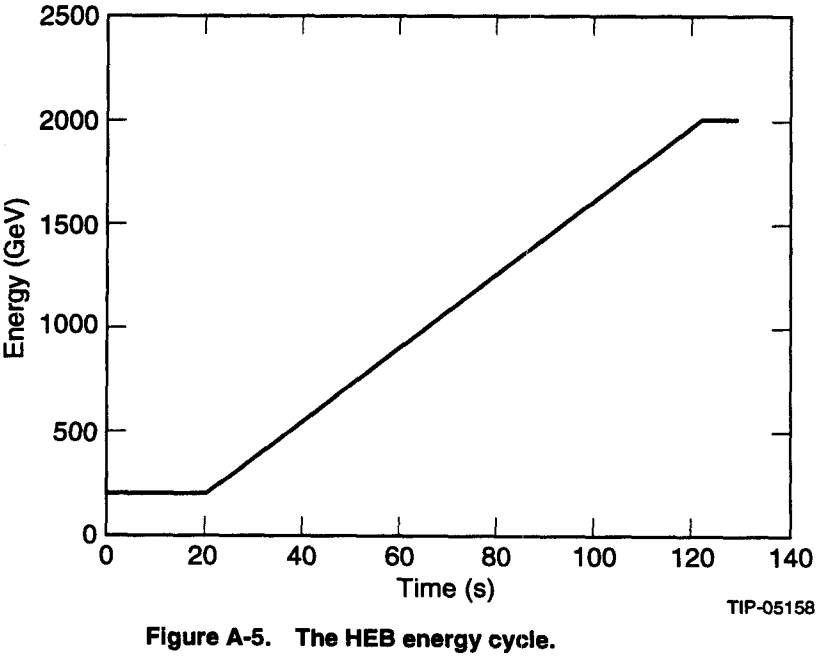

Figure A-5. The HEB energy cycle.

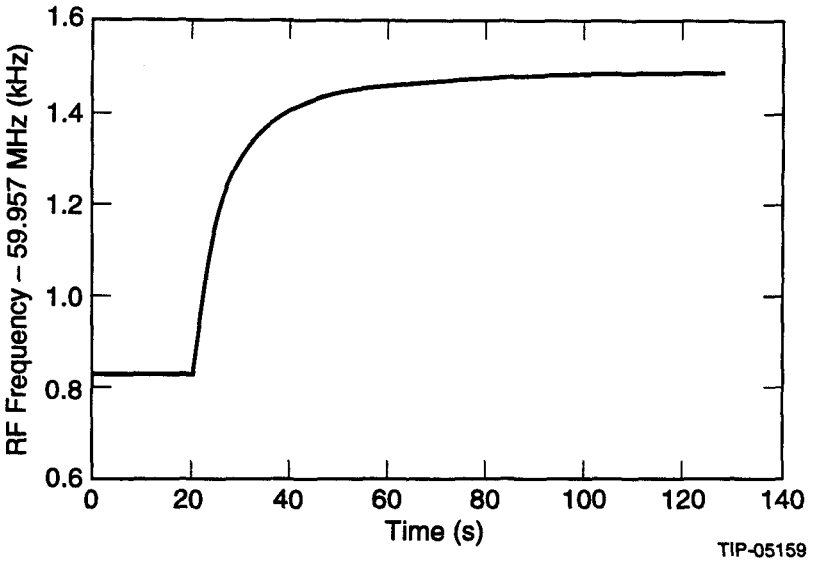

Figure A-6. The HEB rf frequency cycle.

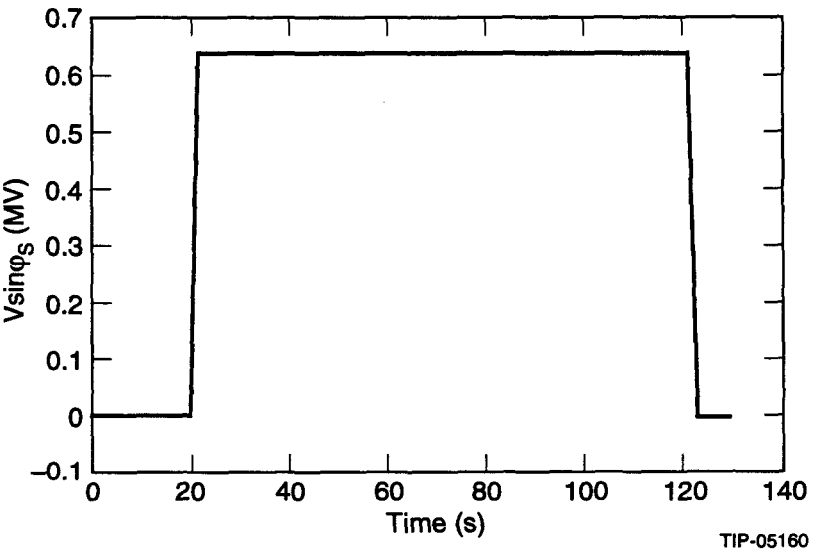

Figure A-7. The HEB $V\sin\varphi_s$ cycle.

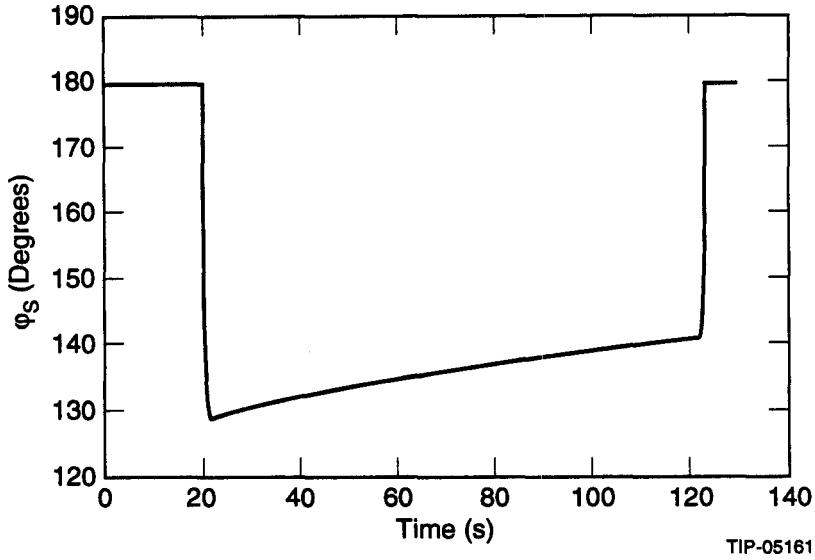

Figure A-8. The HEB φ_s cycle.

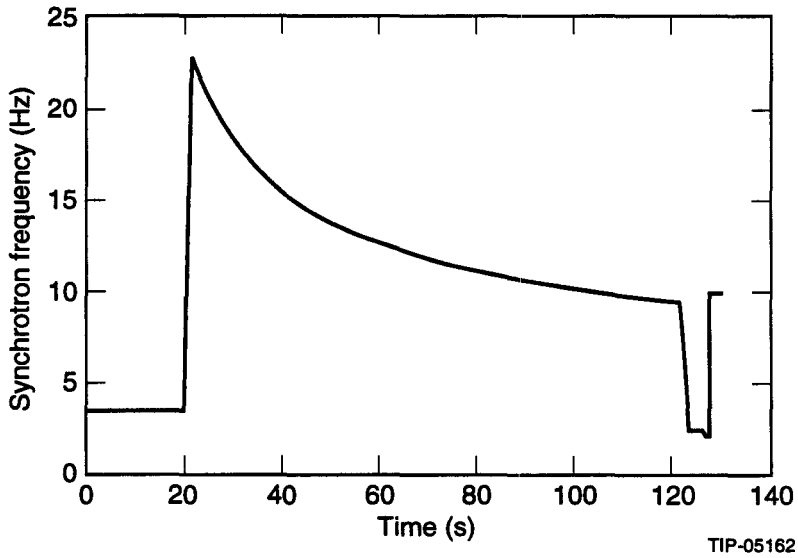

Figure A-9. The HEB synchrotron frequency cycle.

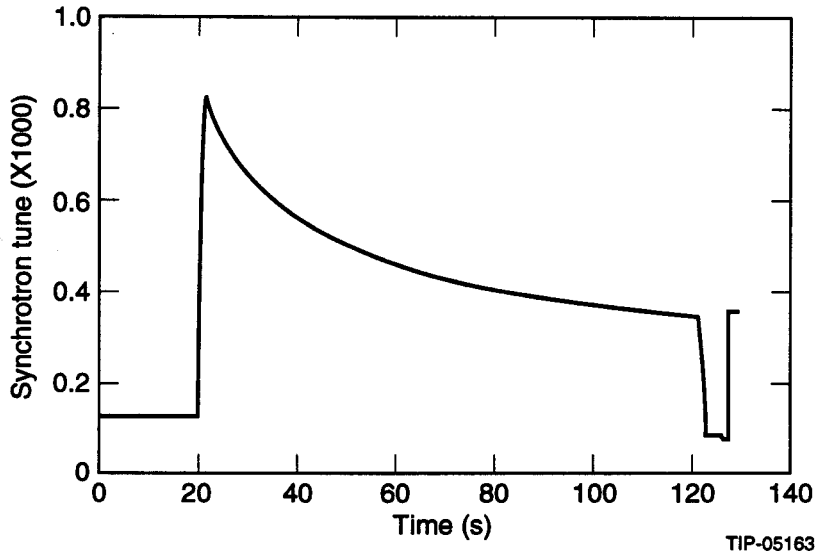

Figure A-10. The HEB synchrotron tune cycle.

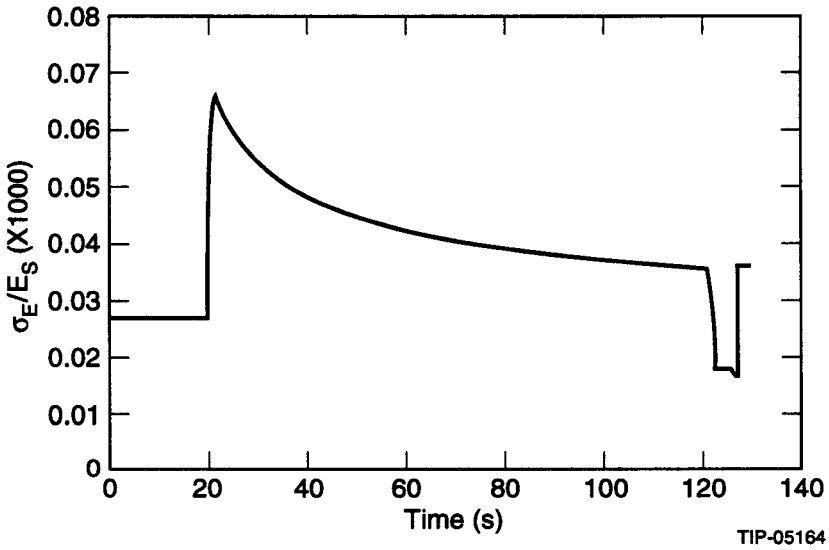

Figure A-11. The HEB σ_E/E_s cycle.

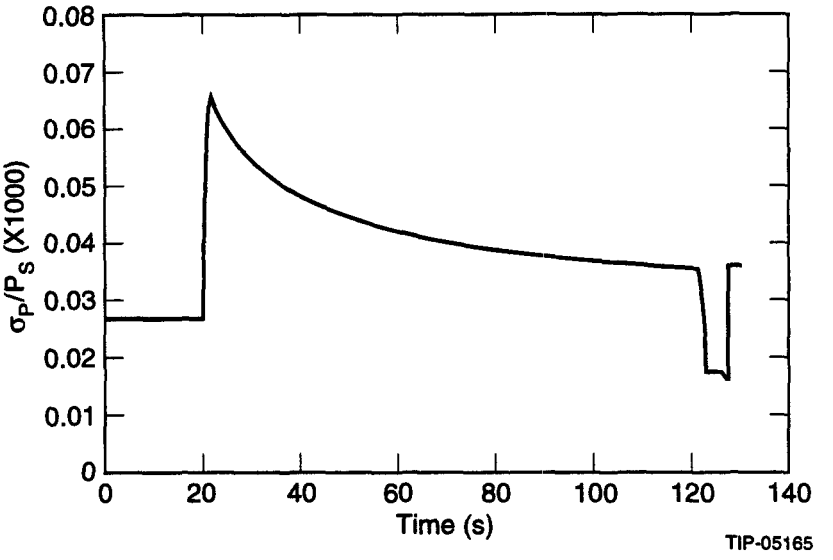

Figure A-12. The HEB σ_P/P_s cycle.

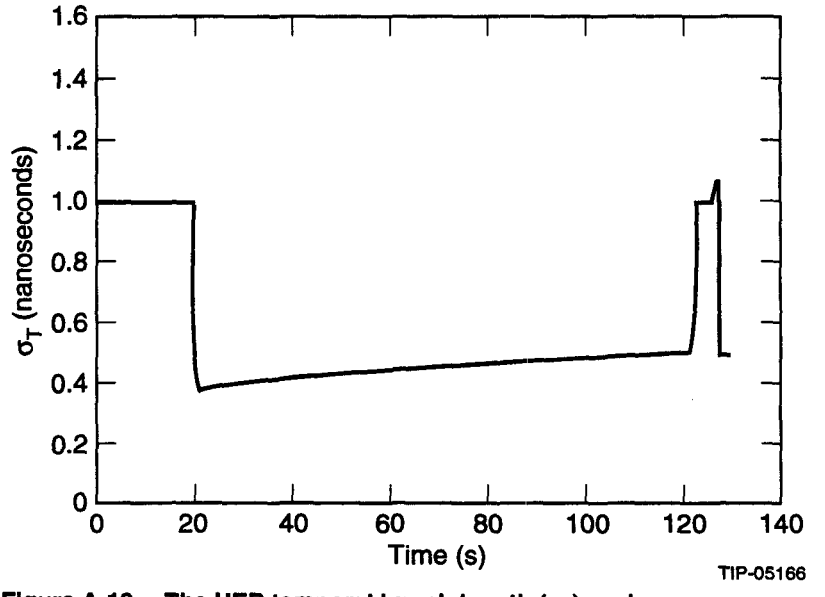

Figure A-13. The HEB temporal bunch length (σ_T) cycle.

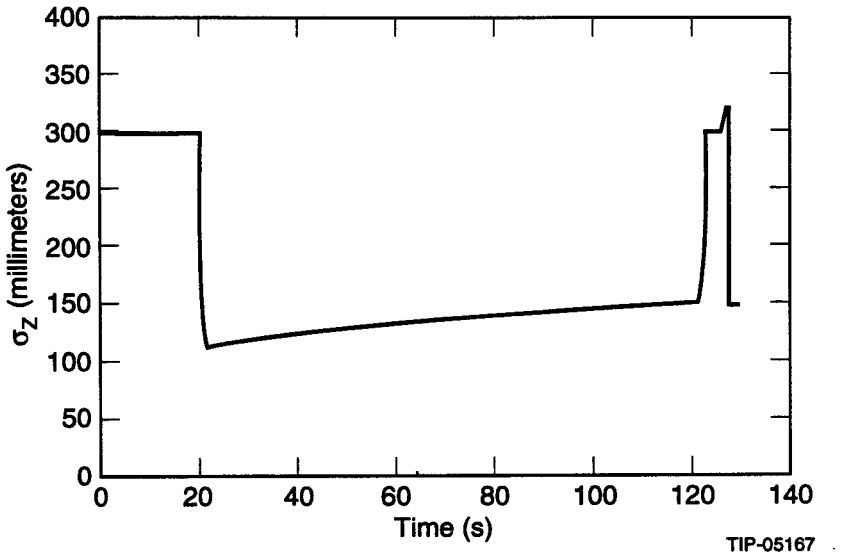

Figure A-14. The HEB spatial bunch length (σ_Z) cycle.

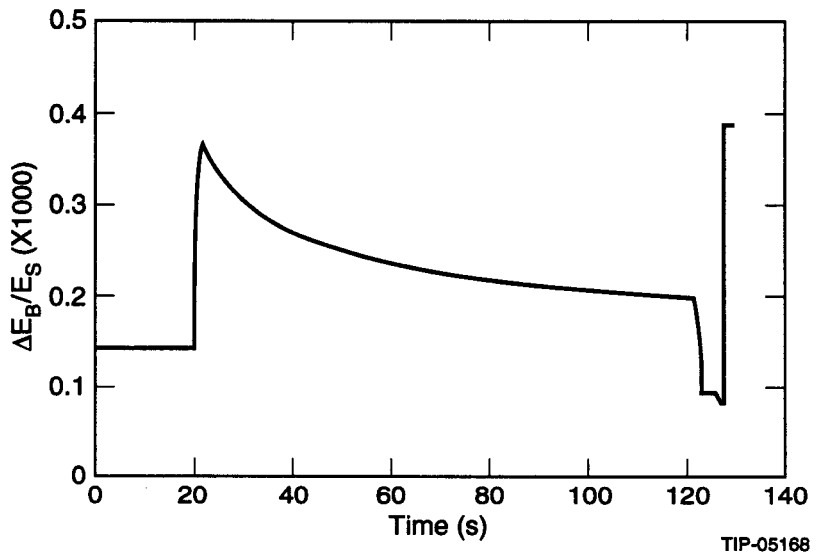

Figure A-15. The HEB relative half bucket height $\Delta E_B/E_S$ cycle.

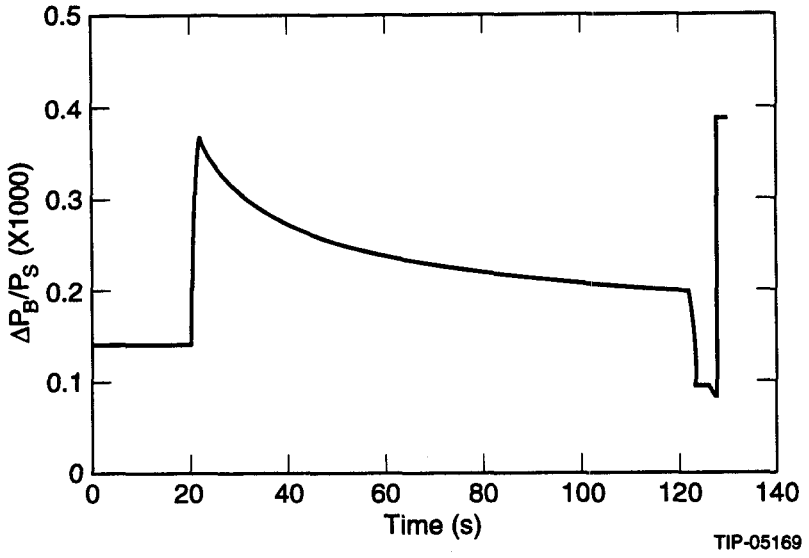

Figure A-16. The HEB relative half bucket height $\Delta P_B/P_S$ cycle.

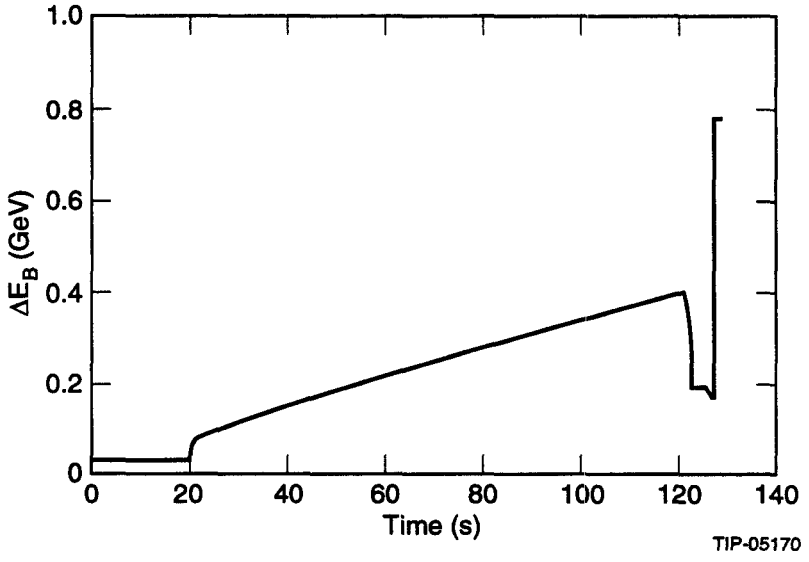

Figure A-17. The HEB half bucket energy height (ΔE_B) cycle.

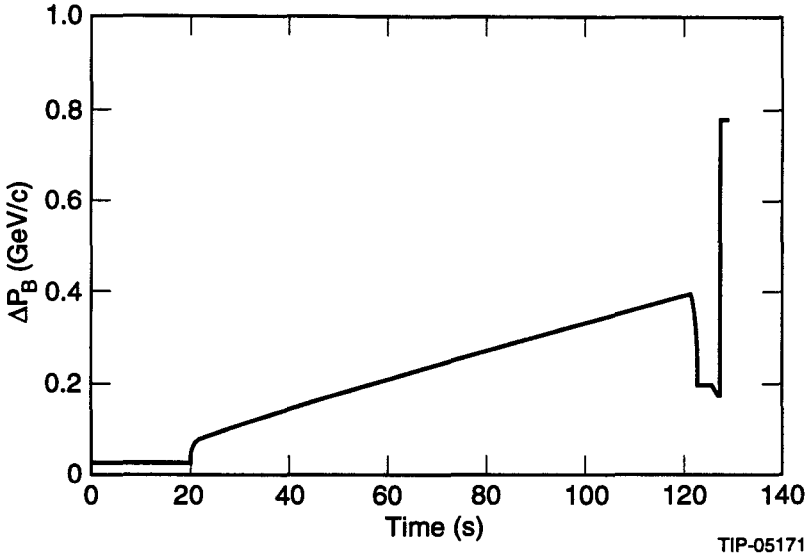

Figure A-18. The HEB half bucket momentum height (ΔP_B) cycle.

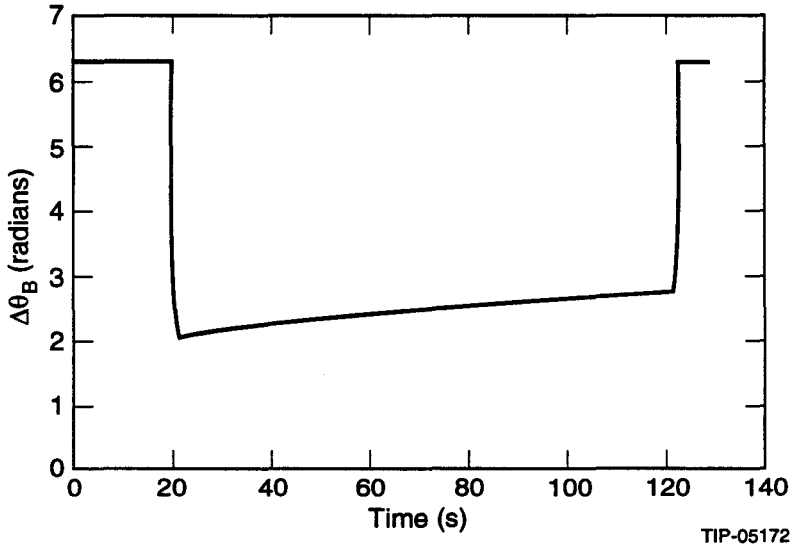

Figure A-19. The HEB full bucket phase width ($\Delta\theta_B$) cycle.

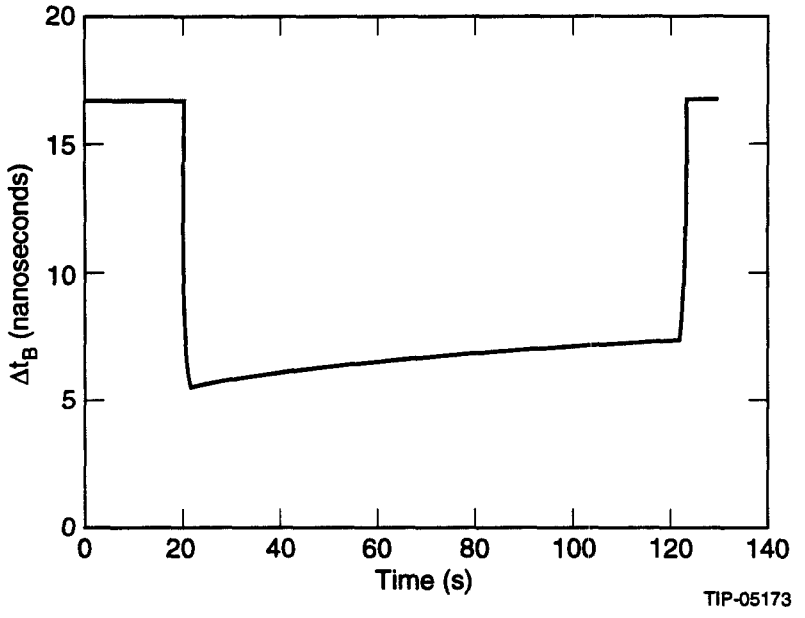

Figure A-20. The HEB full bucket temporal width (Δt_B) cycle.

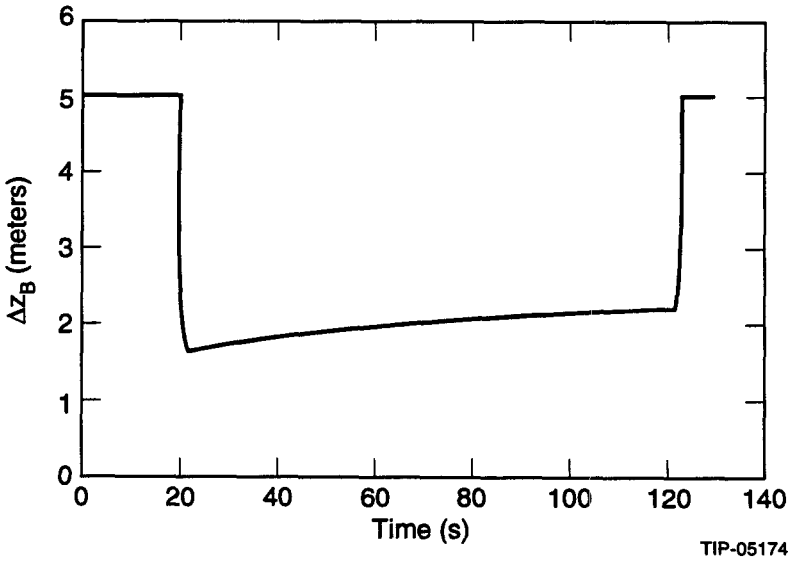

Figure A-21. The HEB full bucket spatial length (ΔZ_B) cycle.

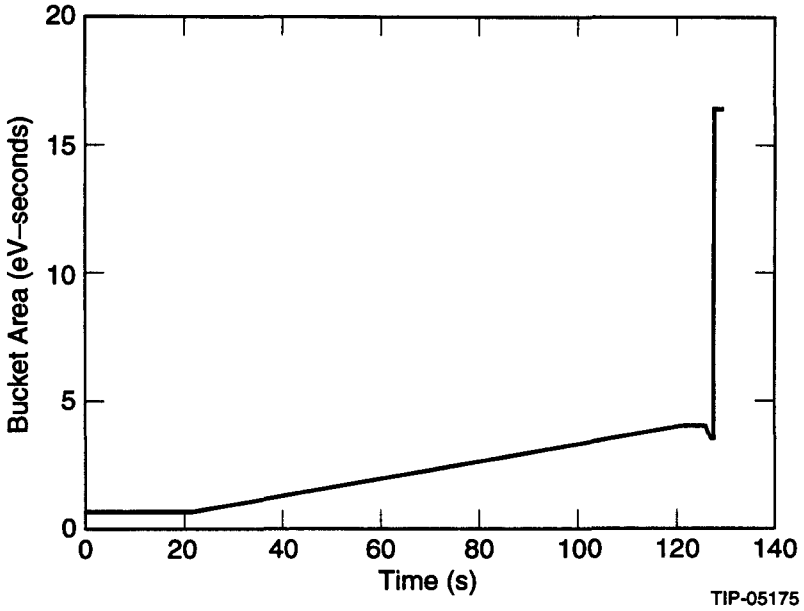

Figure A-22. The HEB bucket area cycle.

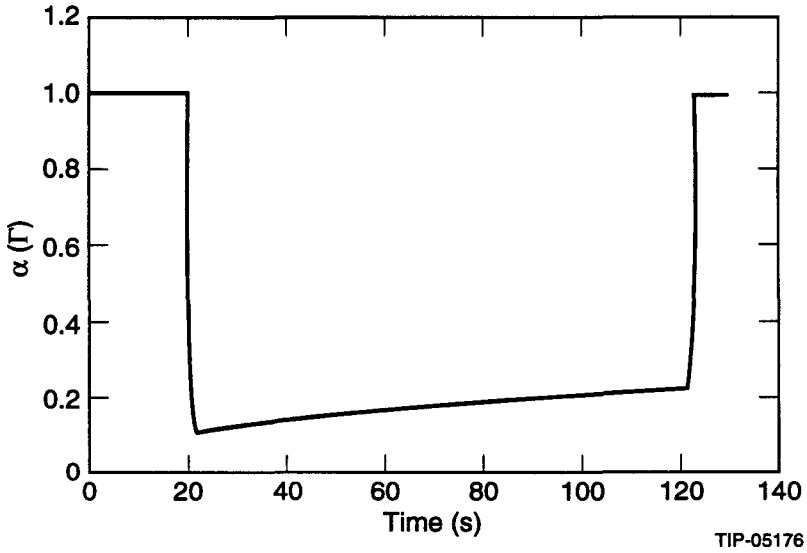

Figure A-23. The HEB α(Γ) cycle.

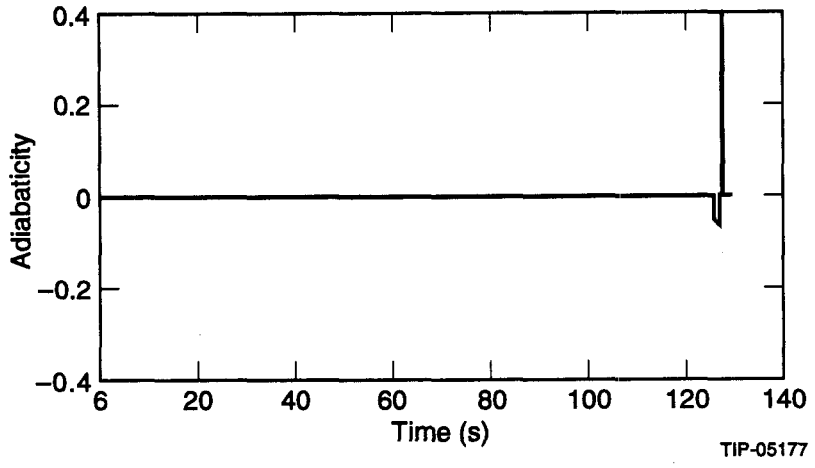

Figure A-24. The HEB adiabaticity cycle.

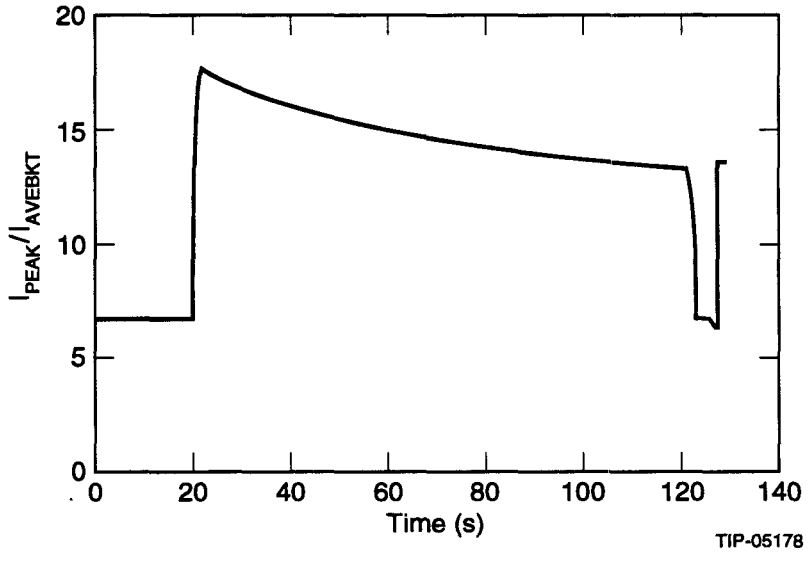

Figure A-25. The HEB bunching factor (I_{PEAK}/I_{AVEBKT}) cycle.

APPENDIX B – SOURCE CODE FOR ELVIRA

```
C       PROGRAM RFHEB
C       This version of ELVIRA is the version referred to in the May 5, 1992
C       writeup, PMTN#0063H.

        INTEGER I,IF1,IFL2,MODE,N,VFLAG

        DIMENSION AA(8)
        DATA AA /1.,-2.423,6.098,-17.53,32.07,-33.6,18.43,-4.05/ ! 7th order fit

        DOUBLE PRECISION ABKT,ABKT0,ABKT1,ABKT2,ABKT3,ABKT4,ABSETA,ABSVSIN
        DOUBLE PRECISION ADIABAT,ALPHA,B,B1,B3,B5,BETA,BF,BKTK,C,CIRC,CONV
        DOUBLE PRECISION DBDT,DEBKT,DEDT,DELTHETA,DENOM,DEOEBNCH,DEOEBKT
        DOUBLE PRECISION DPBKT,DPOPBKT,DPOPBNCH,DT,ENRG,EPL,EPL1,EPL2,ETA
        DOUBLE PRECISION F0,FRF,FS,G,GAMMA,GAMMAT,GFUN,H,MP,NUS,P,P1,P2
        DOUBLE PRECISION P3,P4,P5,P6,PDUM,PHIS,PI,PIO2,Q,QUARTIC,R1,R2
        DOUBLE PRECISION R3,RHO,ROOT,T,T1,T2,T3,T4,T5,T6,T7,T8,T9,T10,T11
        DOUBLE PRECISION T12,TBKT,TBNCH,TCYC,THETA1,THETA2,THETAD,THETAS
        DOUBLE PRECISION TIN1,TIN2,TIN3,TIN4,TIN5,TIN6,TV1,TV2,TV3,TV4
        DOUBLE PRECISION TVIN1,TVIN2,TVIN3,TVIN4,V,V1,V2,V3,V4
        DOUBLE PRECISION VSINPHIS,ZBKT,ZBNCH

0001    Q=1.60217733E-19
0002    C=2.99792458E8
0003    MP=1.6726231E-27
0004    PI=3.141592653589793238
0005    PIO2=PI/2

0006    CONV=1./(Q*1.E9)

0010    OPEN (UNIT=10,STATUS='OLD',FILE='ELVIRA.IN')
        READ (10,*) RHO,GAMMAT,H,CIRC
        READ (10,*) DT,MODE,VFLAG
        READ (10,*) TIN1,P1,B1,TIN2,P2
        READ (10,*) TIN3,P3,B3,TIN4,P4
        READ (10,*) TIN5,P5,B5,TIN6,P6
        READ (10,*) TVIN1,TVIN2,TVIN3,TVIN4
        READ (10,*) V1,V2,V3,V4
        READ (10,*) ABKT1,ABKT2,ABKT3,ABKT4
        READ (10,*) EPL1,EPL2
        CLOSE (10)

0030    OPEN (UNIT=30,STATUS='NEW',FILE='b.dat')
        OPEN (UNIT=31,STATUS='NEW',FILE='v.dat')
        OPEN (UNIT=32,STATUS='NEW',FILE='epl.dat')
        OPEN (UNIT=33,STATUS='NEW',FILE='p.dat')
        OPEN (UNIT=34,STATUS='NEW',FILE='e.dat')
0035    OPEN (UNIT=35,STATUS='NEW',FILE='rf.dat')
        OPEN (UNIT=36,STATUS='NEW',FILE='vsinphis.dat')
```

```
      OPEN (UNIT=37,STATUS='NEW',FILE='phis.dat')
      OPEN (UNIT=38,STATUS='NEW',FILE='fs.dat')
      OPEN (UNIT=39,STATUS='NEW',FILE='nus.dat')
0040  OPEN (UNIT=40,STATUS='NEW',FILE='deoebnch.dat')
      OPEN (UNIT=41,STATUS='NEW',FILE='dpopbnch.dat')
      OPEN (UNIT=42,STATUS='NEW',FILE='tbnch.dat')
      OPEN (UNIT=43,STATUS='NEW',FILE='zbnch.dat')
      OPEN (UNIT=44,STATUS='NEW',FILE='deoebkt.dat')
0045  OPEN (UNIT=45,STATUS='NEW',FILE='dpopbkt.dat')
      OPEN (UNIT=46,STATUS='NEW',FILE='debkt.dat')
      OPEN (UNIT=47,STATUS='NEW',FILE='dpbkt.dat')
      OPEN (UNIT=48,STATUS='NEW',FILE='radbkt.dat')
      OPEN (UNIT=49,STATUS='NEW',FILE='tbkt.dat')
0050  OPEN (UNIT=50,STATUS='NEW',FILE='zbkt.dat')
      OPEN (UNIT=51,STATUS='NEW',FILE='abkt.dat')
      OPEN (UNIT=52,STATUS='NEW',FILE='alpha.dat')
      OPEN (UNIT=53,STATUS='NEW',FILE='adiabat.dat')
      OPEN (UNIT=54,STATUS='NEW',FILE='bf.dat')
      OPEN (UNIT=55,STATUS='NEW',FILE='zon.dat')
      OPEN (UNIT=56,STATUS='NEW',FILE='zperp.dat')

0060  IF1=-1
      IFL2=-1

      T1=TIN1
      T2=T1+P1
      T3=T2+TIN2
      T4=T3+P2
      T5=T4+TIN3
      T6=T5+P3
      T7=T6+TIN4
      T8=T7+P4
      T9=T8+TIN5
      T10=T9+P5
      T11=T10+TIN6
      T12=T11+P6
      T=0.
      TCYC=T5

      TV1=T4+TVIN1
      TV2=T4+TVIN1+TVIN2
      TV3=T4+TVIN1+TVIN2+TVIN3
      TV4=T4+TVIN1+TVIN2+TVIN3+TVIN4

0100  CONTINUE

      R1=(B3-B1)/(TIN2+(P1/2)+(P2/2))
      R2=(B5-B3)/(TIN4+(P3/2)+(P4/2))
      R3=(-B1-B5)/(TIN6+(P5/2)+(P6/2))
```

```
0120        CONTINUE

            IF (T.LT.T1) THEN
            B=B1
            EPL=EPL1
            ABKT=ABKT1
            V=V1
            DBDT=0.
            ENDIF

            IF (T.GE.T1.AND.T.LT.T2) THEN
            B=B1+(R1/(2*(T2-T1)))*(T-T1)**2
            DBDT=(R1/(T2-T1))*(T-T1)
            EPL=EPL1
            ABKT=ABKT1
            V=V1+((V2-V1)/(T2-T1))*(T-T1)
            ENDIF

            IF (T.GE.T2.AND.T.LT.T3) THEN
            B=B1+R1*(T-(.5*T1)-(.5*T2))
            EPL=EPL1+((EPL2-EPL1)/(T3-T2))*(T-T2)
            ABKT=ABKT1+((ABKT2-ABKT1)/(T3-T2))*(T-T2)
            V=V2
            DBDT=R1
            ENDIF

            IF (T.GE.T3.AND.T.LT.T4) THEN
            B=B3+(R1/(2*(T3-T4)))*(T-T4)**2
            EPL=EPL2
            DBDT=(R1/(T3-T4))*(T-T4)
            ABKT=ABKT2
            V=V2
            ENDIF

            IF (T.GE.T4.AND.T.LT.T5) THEN
            B=B3
            EPL=EPL2
            ABKT=ABKT2
            V=V2
            DBDT=0.
            IF (T.LT.TV1) THEN
            ABKT=ABKT2
            V=V2
            ENDIF
                        IF (T.LT.TV2.AND.T.GE.TV1) THEN
                        ABKT=ABKT2+((ABKT3-ABKT2)/(TV2-TV1))*(T-TV1)
                        V=V2+((V3-V2)/(TV2-TV1))*(T-TV1)
                        ENDIF
                        IF (T.LT.TV3.AND.T.GE.TV2) THEN
                        ABKT=ABKT3
                        V=V3
                        ENDIF
                        IF (T.LT.TV4.AND.T.GE.TV3) THEN
                        ABKT=ABKT3+((ABKT4-ABKT3)/(TV4-TV3))*(T-TV3)
```

```
                    V=V3+((V4–V3)/(TV4–TV3))*(T–TV3)
                    ENDIF
                    IF (T.GE.TV4) THEN
                    ABKT=ABKT4
                    V=V4
                    ENDIF
          ENDIF

0200      CONTINUE

          IF (T.GE.T5.AND.T.LT.T6) THEN
          B=B3+(R2/(2*(T6–T5)))*(T–T5)**2
          DBDT=R2*(T–T5)/(T6–T5)
          ENDIF

          IF (T.GE.T6.AND.T.LT.T7) THEN
          B=B3+R2*(T–.5*T5–.5*T6)
          DBDT=R2
          ENDIF

          IF (T.GE.T7.AND.T.LT.T8) THEN
          B=B5+(R2/(2*(T7–T8)))*(T–T8)**2
          DBDT=R2*(T–T8)/(T7–T8)
          ENDIF

          IF (T.GE.T8.AND.T.LT.T9) THEN
          B=B5
          DBDT=0.
          ENDIF

          IF (T.GE.T9.AND.T.LT.T10) THEN
          B=B5+(R3/(2*(T10–T9)))*(T–T9)**2
          DBDT=R2*(T–T9)/(T10–T9)
          ENDIF

          IF (T.GE.T10.AND.T.LT.T11) THEN
          B=B5+R3*(T–.5*T9–.5*T10)
          DBDT=R3
          ENDIF

          IF (T.GE.T11.AND.T.LT.T12) THEN
          B=–B1+(R3/(2*(T11–T12)))*(T–T12)**2
          DBDT=R3*(T–T12)/(T11–T12)
          ENDIF

0240      WRITE (30,*) B,T

0250      CONTINUE

0260      IF (T.LT.TCYC) THEN

0270      IF (VFLAG.LT.0) THEN
0280      WRITE (51,*) ABKT,T
0290      ABKT=Q*ABKT
```

```
0300        ELSE
0310        PDUM=V/1E6
0320        WRITE (31,*) PDUM,T
0330        ENDIF

0340        WRITE (32,*) EPL,T
0345        EPL=EPL*Q

0350        P=Q*B*RHO
0360        PDUM=P*C*CONV
0370        WRITE (33,*) PDUM,T

0380        ENRG=((P*C)**2+(MP**2)*(C**4))**0.5
0390        PDUM=ENRG*CONV
0400        WRITE (34,*) PDUM,T

0410        GAMMA=ENRG/(MP*C**2)
0420        BETA=(1-(1/GAMMA**2))**0.5
0430        DEDT=BETA*C*Q*RHO*DBDT

0440        F0=BETA*C/CIRC
0450        FRF=H*F0
0460        PDUM=(FRF-59957000.)/1000.
0470        WRITE (35,*) PDUM,T

0480        VSINPHIS=DEDT/(Q*F0)
0490        PDUM=VSINPHIS/1E6
0500        WRITE (36,*) PDUM,T

0510        ETA=GAMMAT**-2-GAMMA**-2
0515        ABSETA=(ETA*ETA)**0.5

0520        IF (VFLAG.LT.0) THEN

0530                G=0.0

0535                ABSVSIN=(VSINPHIS*VSINPHIS)**0.5
0540                IF (ABSVSIN.LT.1.) THEN
0550                V=(((ABKT*PI*FRF)/(BETA))**2)*((ABSETA*H*PI)/(32*Q*ENRG))
0555                ALPHA=1.
0560                GOTO 0680
0570                ENDIF

0580                ROOT=((PI*H*ABSETA)/(32*Q*VSINPHIS*ENRG))**0.5
0590                BKTK=((ABKT*PI*FRF)/(BETA))*ROOT

0600                DO 0640 N=1,1000
0610                G=G+0.001
0620                GFUN=((1-G**0.79)**1.27)/(G**0.5)
0630                IF (GFUN.LT.BKTK) GOTO 0650
0640                CONTINUE
0650                V=VSINPHIS/G
```

```
0660                    CONTINUE

0670                    ALPHA=GFUN*G**0.5
0680                    WRITE (52,*) ALPHA,T

0690                    PDUM=V/1E6
0700                    WRITE (31,*) PDUM,T

0710          ELSE

0720                    G=VSINPHIS/V
0730                    ALPHA=AA(1)
0740                    DO 0760 I=2,8
0750                    ALPHA=ALPHA+AA(I)*G**(I-1)
0760                    CONTINUE
0770          ABKT=((BETA*ALPHA)/(PI*FRF))*(((32*ENRG*Q*V)/(H*PI*ABSETA))**0.5)
0780                    PDUM=ABKT/Q
0790                    WRITE (51,*) PDUM,T
0800                    WRITE (52,*) ALPHA,T

0810          ENDIF

0820          IF (GAMMA.GT.GAMMAT) THEN
0830                    PHIS=PI-ASIN(G)
0840          ELSE
0850                    PHIS=ASIN(G)
0860          ENDIF
0870          PDUM=PHIS*180./PI
0880          WRITE (37,*) PDUM,T

0890          FS=(F0/BETA)*(((-1.*H*ETA*Q*V*COS(PHIS))/(2*PI*ENRG))**0.5)
0900          WRITE (38,*) FS,T

0910          NUS=FS/F0
0915          PDUM=1000*NUS
0920          WRITE (39,*) PDUM,T

0930          QUARTIC=((-2.*PI*H*Q*V*COS(PHIS))/(ENRG*ETA))**0.25
0940          DEOEBNCH=(((F0*BETA*EPL)/(6.*PI*ENRG))**0.5)*QUARTIC
0950          PDUM=1000.*DEOEBNCH
0960          WRITE (40,*) PDUM,T

0970          DPOPBNCH=(BETA**-2)*DEOEBNCH
0980          PDUM=1000.*DPOPBNCH
0990          WRITE (41,*) PDUM,T

1000          TBNCH=EPL/(6*PI*(ENRG)*DEOEBNCH)
1010          PDUM=1.E9*TBNCH
1020          WRITE (42,*) PDUM,T

1030          ZBNCH=BETA*C*TBNCH
1040          PDUM=1000*ZBNCH
1050          WRITE (43,*) PDUM,T
```

```
1070        IF (PHIS.LT.0) THETAS=-PHIS
1080        IF (PHIS.LT.PIO2.AND.PHIS.GE.0) THETAS=PHIS
1090        IF (PHIS.LT.PI.AND.PHIS.GE.PIO2) THETAS=PI-PHIS
1100        IF (PHIS.GE.PI) THETAS=PHIS-PI

1110        DENOM=(PI*H*ABSETA*ENRG)/(Q*V*BETA**2)
1120        DEOEBKT=((2*COS(THETAS)+(2*THETAS-PI)*SIN(THETAS))/DENOM)**0.5
1130        PDUM=1000*DEOEBKT
1140        WRITE (44,*) PDUM,T

1150        DPOPBKT=DEOEBKT/(BETA**2)
1160        PDUM=1000*DPOPBKT
1170        WRITE (45,*) PDUM,T

1180        DEBKT=DEOEBKT*ENRG
1190        PDUM=CONV*DEBKT
1200        WRITE (46,*) PDUM,T

1210        DPBKT=DPOPBKT*P
1220        PDUM=CONV*DPBKT*C
1230        WRITE (47,*) PDUM,T

1240        THETA2=PI-THETAS
1250        THETAD=180.*THETAS/PI
1260        THETA1=((THETAD**0.5)*(25.809-3.351*G+7.050*G*G))-180.
1270        IF (G.GT.0.45) THEN
1280        THETA1=((THETAD**0.5)*(25.761-1.784*G+3.717*G*G))-180.
1290        ENDIF
1300        IF (G.GT.0.9) THEN
1310        THETA1=(2*THETAD*(1.-0.0657*G+0.0677*G*G))-90.
1320        ENDIF
1330        THETA1=THETA1*PI/180.
1340        DELTHETA=THETA2-THETA1
1350        WRITE (48,*) DELTHETA,T

1360        TBKT=DELTHETA/(2*PI*FRF)
1370        PDUM=1E9*TBKT
1380        WRITE (49,*) PDUM,T

1390        ZBKT=BETA*C*TBKT
1410        WRITE (50,*) ZBKT,T

1420        IF (IFL2.LT.0) THEN
1430                    IFL2=1
1440                    ABKT0=ABKT
1450        ELSE
1460                    ADIABAT=(ABKT-ABKT0)/(0.5*(ABKT+ABKT0)*DT*FS)
1470                    ABKT0=ABKT
1480                    WRITE (53,*) ADIABAT,T
1490        ENDIF

1500        BF=(BETA*C)/(FRF*ZBNCH*((2*PI)**0.5))
```

```
1510        WRITE (54,*) BF,T

            ENDIF

            T=T+DT
            IF (MODE.EQ.1.AND.T.GT.T8) GOTO 9999
            IF (MODE.EQ.2.AND.T.GT.T12) THEN
                        IF (IF1.LT.0) THEN
                        IF1=1
                        T1=T1+T12
                        T2=T2+T12
                        T3=T3+T12
                        T4=T4+T12
                        T5=T5+T12
                        T6=T6+T12
                        T7=T7+T12
                        T8=T8+T12
                        T9=T9+T12
                        T10=T10+T12
                        T11=T11+T12
                        T12=T12+T12
                        B1=-B1
                        B3=-B3
                        B5=-B5
                        GOTO 0100
                        ENDIF
                        GOTO 9999
1700        ENDIF
2000        GOTO 0120
9999        CONTINUE

            CLOSE (30)
            CLOSE (30)
            CLOSE (31)
            CLOSE (32)
            CLOSE (33)
            CLOSE (34)
            CLOSE (35)
            CLOSE (36)
            CLOSE (37)
            CLOSE (38)
            CLOSE (39)
            CLOSE (40)
            CLOSE (40)
            CLOSE (41)
            CLOSE (42)
            CLOSE (43)
            CLOSE (44)
            CLOSE (45)
            CLOSE (46)
            CLOSE (47)
            CLOSE (48)
            CLOSE (49)
            CLOSE (50)
```

```
CLOSE (51)
CLOSE (52)
CLOSE (53)
CLOSE (54)
CLOSE (55)
CLOSE (56)
STOP
END
```